Sedimentary Geology 300 (2014) 28–48

Contents lists available at ScienceDirect

Sedimentary Geology

journal homepage: www.elsevier.com/locate/sedgeo

Lower Triassic mixed carbonate and siliciclastic setting with Smithian–Spathian anoxic to dysoxic facies, An Chau basin, northeastern Vietnam

Toshifumi Komatsu [a,*], Hajime Naruse [b], Yasunari Shigeta [c], Reishi Takashima [d], Takumi Maekawa [a], Huyen T. Dang [e], Tien C. Dinh [e], Phong D. Nguyen [e], Hung H. Nguyen [f], Gengo Tanaka [g], Masatoshi Sone [h]

[a] Graduate School of Science and Technology, Kumamoto University, Kumamoto 806-8555, Japan
[b] Graduate School of Science, Kyoto University, Kyoto 606-8502, Japan
[c] Department of Geology and Paleontology, National Museum of Nature and Science, 4-1-1 Amakubo, Tsukuba, Ibaraki 305-0005, Japan
[d] The Center for Academic Resources and Archives Tohoku University Museum, Tohoku University, Aramaki Aza Aoba 6-3, Aoba-ku, Sendai 980-8578, Japan
[e] Vietnam Institute of Geosciences and Mineral Resources (VIGMR), Hanoi, Viet Nam
[f] Vietnam National Museum of Nature (VNMN), Hanoi, Viet Nam
[g] Japan Agency for Marine-Earth Science and Technology, 2-15 Natsushima, Yokosuka City, Kanagawa 237-0061, Japan
[h] Department of Geology, Faculty of Science, University of Malaya 50603 Kuala Lumpur, Malaysia

ARTICLE INFO

Article history:
Received 15 August 2013
Received in revised form 29 October 2013
Accepted 29 October 2013
Available online 6 November 2013

Editor: B. Jones

Keywords:
Anoxic to dysoxic facies
Depositional environment
Lower Triassic
Nanpanjiang basin
Smithian–Spathian boundary
Tethys

ABSTRACT

In the An Chau basin in northeastern Vietnam, the Olenekian (Lower Triassic) stage comprises mixed carbonate and siliciclastic shallow marine to marginal basin deposits that extend into the southern Nanpanjiang basin in South China. The upper Lang Son Formation, which is dominated by siliciclastic facies, is composed of storm- and wave-influenced shallow marine and slope deposits. The overlying and interfingering Bac Thuy Formation consists of tidal flat, wave-influenced carbonate platform, slope, and marginal basin plain deposits. The tidal flat deposits are composed mainly of lenticular, wavy-bedded, or thin flat-bedded carbonates containing desiccation cracks and ripples that are indicative of bidirectional paleocurrents. The platform carbonates are characterized by wave ripples, ooids, and abundant marine mollusks and microfossils; the molluscan fossil assemblage primarily contains Smithian ammonoids such as *Owenites koeneni*. The slope deposits are characterized by limestone breccia and slump beds. The marginal basin plain deposits consist of classical turbidite beds, minor limestone breccia, and hemipelagic mudstone and marl containing the Spathian ammonoids *Tirolites* and *Columbites*. The turbidite sets may represent frontal splay environments in the marginal basin plain. These Olenekian carbonate and siliciclastic facies are typical of a transgressive succession.

The Smithian–Spathian boundary and the anoxic to dysoxic facies of the latest Smithian are characterized by organic-rich dark gray limestone and mudstone deposits intercalated in the succession of slope to marginal basin plain facies, which are composed mainly of gravity flow and hemipelagic deposits. The organic-rich deposits show no evidence of bioturbation and are characterized by low-diversity fauna. Clastics in the marginal basin plain deposits were apparently supplied from the west; hence, the paleocurrent direction of the siliciclastic gravity flows was approximately eastward.

1. Introduction

In northeastern Vietnam, Paleozoic to Mesozoic deposits are widely exposed in the An Chau basin (Fig. 1), and they extend into the southern Nanpanjiang basin in South China. These deposits are important for regional correlations and reconstructions of Early Triassic depositional environments, tectonics, biofacies, and marine ecosystems in the eastern Tethys seaway during the recovery interval after the end-Permian mass extinction. The Yangtze platform and several large isolated carbonate platforms, which are distributed on the South China block in Vietnam and China and are surrounded by Nanpanjiang basin deposits, developed during the Early Triassic (Bao, 1998; Lehrmann et al., 1998, 2001, 2003; Komatsu et al., 2004, 2006; Lehrmann et al., 2007a,b; Galfetti et al., 2008; Komatsu et al., 2010; Li et al., 2012). Lehrmann et al. (2001, 2003, 2007a,b) and Galfetti et al. (2008) have reported in detail on the lithofacies and depositional environments of these isolated platforms and hemipelagic basin deposits in the Nanpanjiang basin in Guangxi Province, South China.

* Corresponding author.
E-mail address: komatsu@sci.kumamoto-u.ac.jp (T. Komatsu).

0037-0738/$ – see front matter.
http://dx.doi.org/10.1016/j.sedgeo.2013.10.009

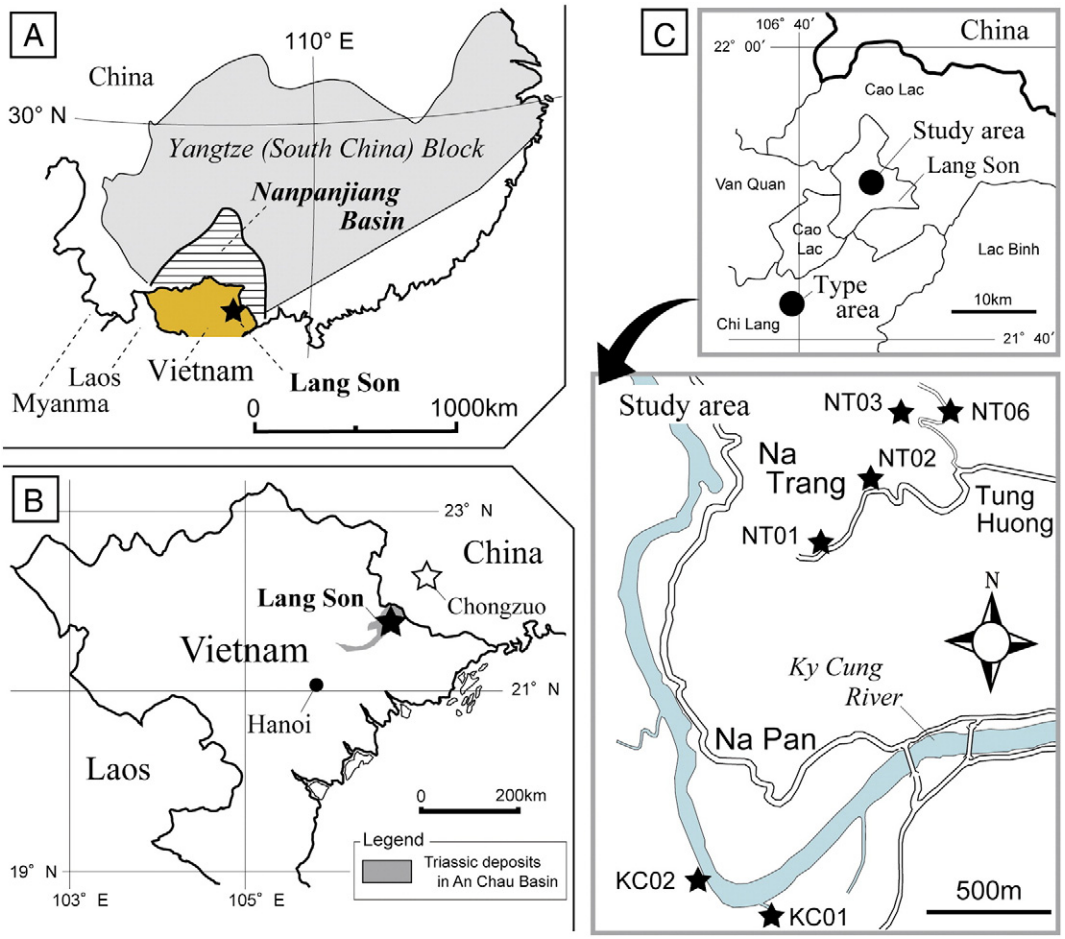

Fig. 1. (A) Locations of the Yangtze (South China) block and Early Triassic Nanpanjiang basin. Modified from Lehrmann et al. (2007). (B) The An Chau depositional basin is located primarily in Lang Son Province, Vietnam. Lower Triassic deposits are widely distributed in northeastern Vietnam and South China. (C) Location of the study area. Black stars show the locations of the studied sections.

In Lang Son Province, northeastern Vietnam (adjacent to Guangxi Province, China), the main formations exposed include the Induan to Olenekian Lang Son Formation and the Olenekian Bac Thuy Formation (Fig. 2; Dang, 1998; Dang and Nguyen, 2005; Dang, 2006). The Lang Son Formation is composed dominantly of siliciclastics containing abundant Induan *Claraia* shell concentrations (Komatsu et al., 2008). The uppermost part of the formation contains rare *Claraia intermedia multistriata* Ichikawa bivalve fossils, indicating deposition in the Induan to Olenekian (Komatsu and Dang, 2007), and also includes Olenekian conodont assemblages (Maekawa et al., 2013). Some units in the upper part of the formation are composed of wave- and storm-dominated shoreface and shelf deposits (Komatsu and Dang, 2007). The overlying Bac Thuy Formation consists mainly of fossiliferous carbonates and hemipelagic deposits. Many studies have described the geology, stratigraphy, and age of this formation (Khuc, 1984; Thang, 1989; Khuc, 1991; Dang, 2006). Recently, Komatsu et al. (2011, 2013) described the bivalve assemblages, the Olenekian ammonoid zones, and the Smithian–Spathian boundary in the Bac Thuy Formation in detail, and preliminary studies of the conodont and ammonoid assemblages and characteristic radiolarian species have been published (Komatsu et al., 2011; Maekawa et al., 2012, 2013). The depositional environments of the Bac Thuy Formation are not well known, however, although excellent exposures provide opportunities for examining well-preserved sedimentary structures in carbonate facies.

In this study, we performed a facies analysis to reconstruct the depositional environments of the upper Lang Son Formation, which is composed mainly of siliciclastic deposits, and the Bac Thuy Formation, which is characterized by carbonates and siliciclastics. The study aimed to improve facies models of carbonate and siliciclastic rocks accumulated by wave, tidal, and sediment gravity flow processes. Thus, this paper is a new case study of a mixed carbonate-siliciclastic system representing shallow marine to marginal basin plain depositional environments. We focus on the slope to marginal basin plain deposits, which record anoxic to dysoxic events of the latest Smithian to earliest Spathian, and on the depositional history

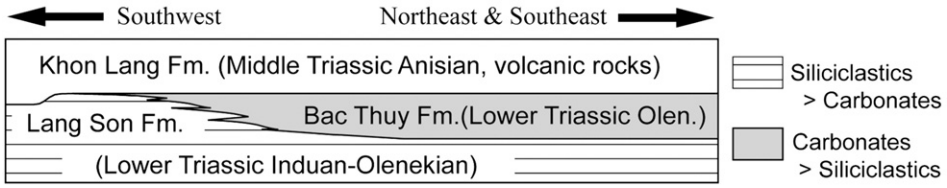

Fig. 2. Stratigraphic relationships in the Lower Triassic system in the An Chau basin, northern Vietnam. The Induan to Olenekian Lang Son Formation is dominated by siliciclastic sediments. The Olenekian Bac Thuy Formation is composed mainly of carbonates and siliciclastics.

of the Olenekian shallow marine, slope, and marginal basin plain deposits in the southern Nanpanjiang basin, northeastern Vietnam.

2. Geologic setting and stratigraphic architecture

The Nanpanjiang basin is a vast, shallow to deep marine embayment in the southern part of the South China block. During the late Permian to Early Triassic, it was located in the eastern Tethys seaway near the equator (Metcalfe, 1998, 2009). According to Metcalfe (2009), the South China block originally rifted and separated from the northern margin of Gondwanaland in the Devonian and drifted northward in the Triassic. The An Chau basin in Vietnam, which is located in the southern part of the South China block, was continuous with the southeastern Nanpanjiang basin during the Triassic. In the southwestern part of Guangxi Province, the Nanpanjiang basin surrounds several large, isolated platforms, including the Chongzuo-Pingguo and Debao platforms (Lehrmann et al., 2007a,b). In the Chongzuo area of southwestern Guangxi Province, the Early Triassic Nanpanjiang basin is filled with mudstone and debris flow deposits of the Luolou Formation (Induan to Olenekian) and with isolated shallow marine platform deposits of the Majiaoling (Induan) and Beisi (Induan to Olenekian) Formations (Lehrmann et al., 2007a,b).

In contrast, the Early Triassic An Chau basin is filled mainly with shallow marine siliciclastics of the Induan to early Olenekian Lang Son Formation. These shallow marine deposits are composed of shoreface sandstone, characterized by wave ripples and hummocky cross-stratification (HCS), and shelf mudstone (Komatsu et al., 2006; Komatsu and Dang, 2007). The top of the formation is either conformably overlain by thick limestone breccias and thin limestone beds of the basal Bac Thuy Formation or unconformably overlain by the Middle Triassic (Anisian) Khon Lang Formation, which is composed mainly of volcanic and siliciclastic rocks (Figs. 2, 3). The Olenekian Bac Thuy Formation consists of fossiliferous carbonates, limestone breccia, and hemipelagic basinal mudstone; it is lithologically equivalent to the Luolou Formation.

In its type area at Bac Thuy, Chi Lang area (Fig. 1), the Bac Thuy Formation is approximately 40 m thick and is composed of alternating beds of limestone and mudstone at the base, overlain by fossiliferous limestone beds and thick mudstone deposits. The bioclastic bedded limestone commonly includes the early Olenekian (Smithian) ammonoids *Flemingites* and *Owenites* (Khuc et al., 1965 Khuc, 1991). The upper part of the formation is composed dominantly of mudstone, which contains abundant bivalves and the late Olenekian (Spathian) ammonoids *Columbites* and *Tirolites*, as well as the latest Smithian to earliest Spathian ammonoid *Xenoceltites variocostatus* Brayard and Bucher (Komatsu et al., 2011).

Dang (2006) described the geologic framework, stratigraphy, and molluscan fossils of the Bac Thuy Formation in the Lang Son area. According to Dang (2006), the Bac Thuy Formation is widespread in this area and attains a total maximum thickness of more than 185 m, which is much thicker than the stratotype at Bac Thuy.

In the Lang Son area, the Bac Thuy Formation conformably overlies the thick mudstone and slump deposits of the Lang Son Formation and is overlain by volcanic rocks of the Anisian Khon Lang Formation. In Na Trang village (sections NT01–NT05), central Lang Son City, the Bac Thuy Formation is approximately 70 m thick and consists mainly of bedded limestone, limestone breccia, and mudstone (Fig. 3). The lower part of the formation is predominantly mudstone, commonly intercalated by carbonate lenses (from approximately 30 m to several hundred meters wide) composed of thick limestone breccias and thin-bedded lime mudstone. The middle section of the formation in this area is characterized by alternating dark gray organic-rich limestone and mudstone with abundant radiolarians, the bivalve *Crittendenia*, the uppermost Smithian to lowermost Spathian ammonoid *X. variocostatus*, and the nautiloid *Trematoceras* sp. (Komatsu et al., 2011, 2013). Komatsu et al. (2013) reported that the organic-rich mudstone commonly includes dark gray calcareous nodules and nodular beds containing thin, densely packed molluscan shell concentrations and abundant radiolarians. In the upper part of the formation, thick gray mudstone bears the Spathian ammonoids *Columbites* and *Tirolites* and the bivalves *Crittendenia*, *Leptochondria*, and *Bositra*. The thick gray mudstone is locally overlain by alternating siliciclastic sandstone and mudstone.

Along the Ky Cung River (sections KC01, KC02) in western Lang Son City, the Bac Thuy Formation is approximately 100 m thick and is divided into lower and upper parts (Fig. 3). The lower part is dominated by carbonates consisting of limestone breccia and bedded limestone with abundant specimens of the Smithian ammonoid *Owenites* (Fig. 4). The upper part consists mainly of thick limestone breccia, bedded lime mudstone, and alternating dark gray organic-rich limestone and mudstone bearing numerous radiolarians and molluscan fossils. The alternating limestone and mudstone beds, which contain the bivalve *Crittendenia* and the ammonoid *X. variocostatus*, are overlain by a thick bed of greenish gray mudstone bearing the Spathian ammonoids *Columbites* and *Tirolites* and the bivalves *Crittendenia*, *Leptochondria*, and *Bositra*.

In Ban Ru (section BR01), northern Chi Lang area, Lang Son Province, the succession in the upper part of the Bac Thuy Formation is lithologically similar to that of the upper Ky Cung River sections (KC02), but the lithology of the lower part of the formation at Ban Ru has not been described. The upper part of the formation at Ban Ru is composed mainly of mudstone, limestone breccia, bedded lime mudstone, and alternating dark gray organic-rich limestone and mudstone containing abundant ostracods (*Propontcypris*), bivalves (*Crittendenia*) and the uppermost Smithian to lowermost Spathian ammonoid *X. variocostatus* (Fig. 3). The alternating limestone and mudstone are overlain by a thick bed of mudstone containing Spathian ammonoids.

In Pac Khanh (PK01), northern Chi Lang area, the succession in the upper part of the Bac Thuy Formation also lithologically resembles that of the upper Ky Cung River sections (KC02). The lower part of the formation at Pac Khanh consists mainly of limestone breccia, bedded limestone and greenish gray mudstone. Abundant Smithian ammonoids (e.g., *Owenites*) are present in these limestones. The lower part of the formation is overlain by thin dark gray organic-rich mudstone containing calcareous nodules. The upper part of the formation is dominated by alternating sandstone and mudstone.

These sections have been regionally correlated on the basis of the first appearance of the diagnostic Spathian ammonoids *Tirolites* and *Columbites* (Fig. 3). These ammonoids have also been reported in South China (Galfetti et al., 2008). In addition, Galfetti et al. (2008) and Brayard and Bucher (2008) described organic-rich shale with nodular limestone containing abundant *Xenoceltites* in Unit IV of the Luolou Formation, southern Guangxi Province, which is dominated by outer platform deposits.

3. Methods

To reconstruct the depositional environments of the Bac Thuy Formation, we performed a facies analysis based on the lithology, sedimentary structures, grain size, paleocurrent data, and fossils of the deposits. Columnar data and rock samples were collected in the Ban Ru (BR01), Pac Khanh (PK01), Ky Cung River (KC01, 02), and Na Trang (NT01–05) areas. In the laboratory, we observed the detailed sedimentary structures and fabrics of block samples from the

Fig. 3. Stratigraphic columns of the upper Lang Son and Bac Thuy Formations in the Lang Son area. The Smithian ammonoids *Owenites* (○) and *Xenoceltites* (☆) and a Spathian ammonoid assemblage (★) consisting of *Tirolites* and *Columbites* are present in the Bac Thuy Formation.

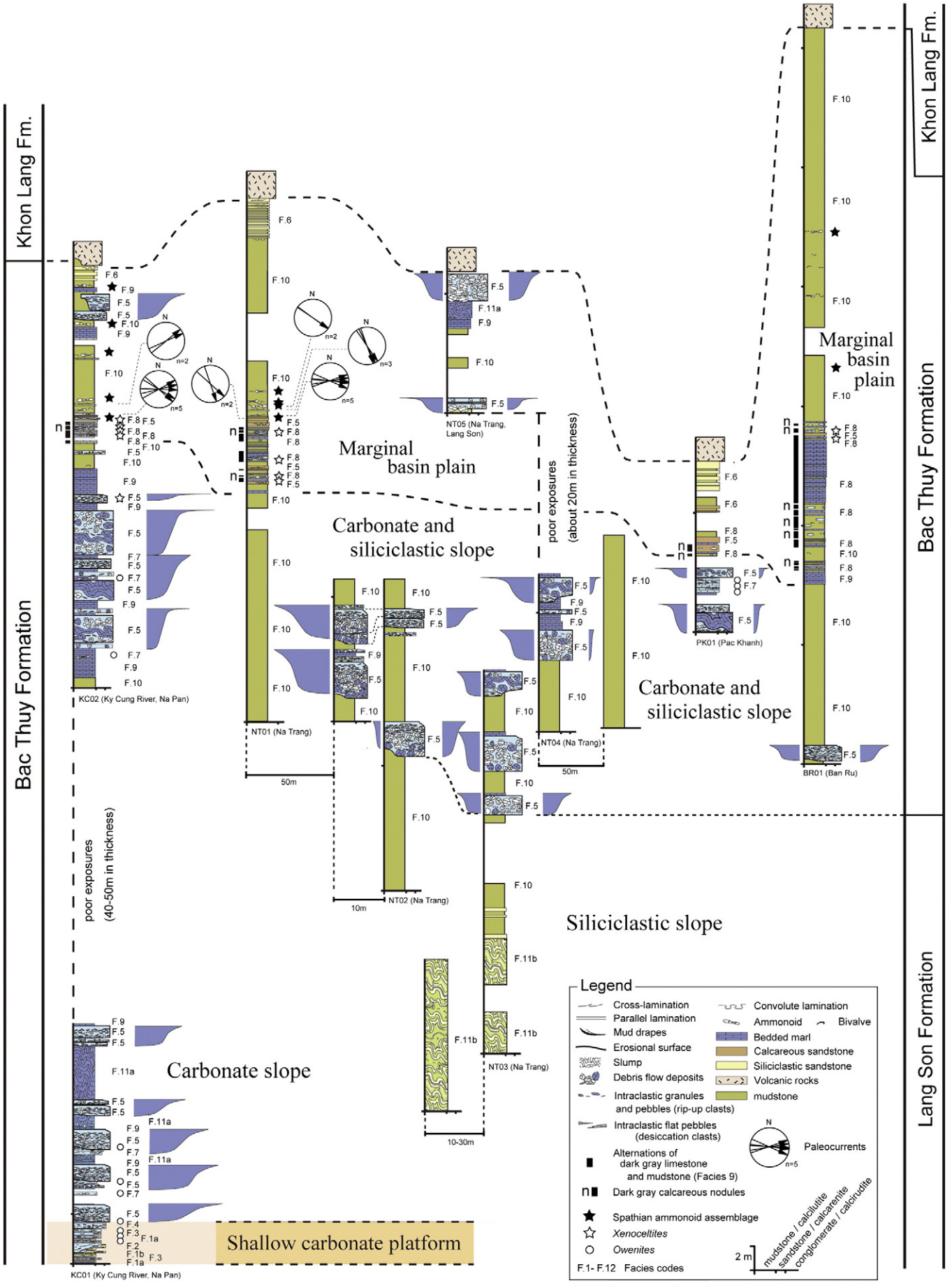
Khon Lang Fm.
Bac Thuy Formation
Khon Lang Fm.
Bac Thuy Formation
Lang Son Formation
Marginal basin plain
Carbonate and siliciclastic slope
poor exposures (about 20m in thickness)
Marginal basin plain
Carbonate and siliciclastic slope
poor exposures (40-50m in thickness)
Siliciclastic slope
Carbonate slope
Shallow carbonate platform
KC02 (Ky Cung River, Na Pan)
NT01 (Na Trang)
NT05 (Na Trang, Lang Son)
PK01 (Pac Khanh)
NT04 (Na Trang)
BR01 (Ban Ru)
NT02 (Na Trang)
NT03 (Na Trang)
KC01 (Ky Cung River, Na Pan)
50m
10m
10-30m
Legend
Cross-lamination
Parallel lamination
Mud drapes
Erosional surface
Slump
Debris flow deposits
Intraclastic granules and pebbles (rip-up clasts)
Intraclastic flat pebbles (desiccation clasts)
Alternations of dark gray limestone and mudstone (Facies 9)
Dark gray calcareous nodules
Spathian ammonoid assemblage
Xenoceltites
Owenites
F.1- F.12 Facies codes
Convolute lamination
Ammonoid
Bivalve
Bedded marl
Calcareous sandstone
Siliciclastic sandstone
Volcanic rocks
mudstone
Paleocurrents
mudstone / calcilutite
sandstone / calcarenite
conglomerate / calcirudite
2 m

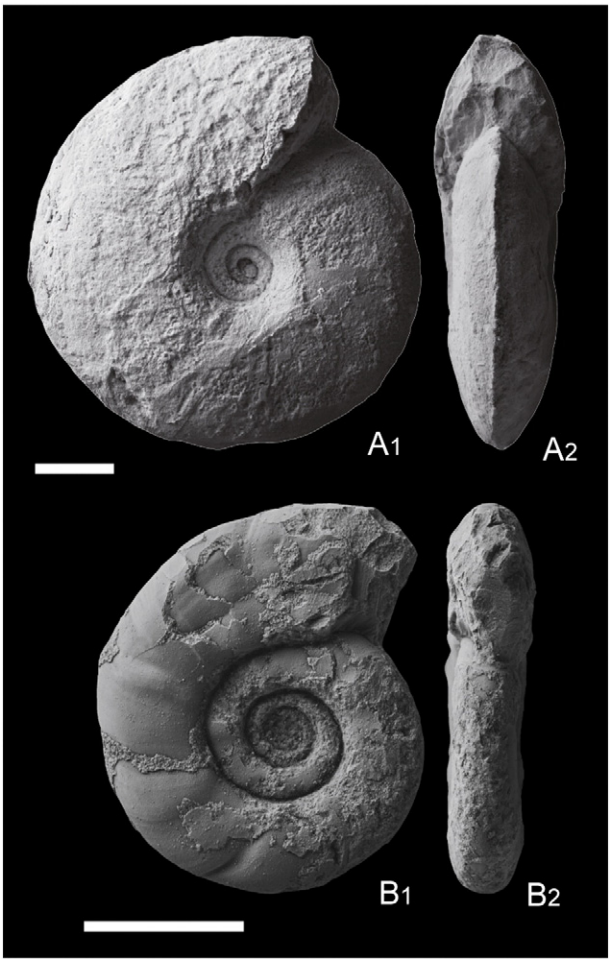

Fig. 4. Olenekian ammonoids from the Bac Thuy Formation. (A) *Owenites koeneni* Hyatt and Smith, from the lower Bac Thuy Formation (section KC01) in lateral (A1) and apertural (A2) views. (B) *Xenoceltites variocostatus* Brayard and Bucher, from the upper Bac Thuy Formation (section NT01) in lateral (B1) and apertural (B2) views. Scale bars represent 1 cm.

sections. In addition, we prepared thin sections for limestone petrographic analysis and observations of microfossils.

Molluscan fossils and bulk rock samples containing shell concentrations were collected bed by bed, and their modes of occurrence were observed in the field. The bulk rock samples were broken up in the laboratory to observe shell preservation and to collect small mollusks. Samples for microfossil analysis, collected mainly from limestone, were processed by the conventional acetic acid and hydrochloric acid techniques. Organic matter and minerals such as quartz and pyrite were also observed in the processed samples. The sedimentological terminology follows that of Tucker and Wright (1990), Tucker (1991), Reading and Collinson (1996), Mulder and Alexander (2001), and Mulder (2011).

4. Facies descriptions and depositional environments

We recognized 11 numbered facies (Figs. 3, 5). In addition, Facies 1 and 11 are each subdivided into two subfacies, Facies 1a and 1b and Facies 11a and 11b, respectively. Facies 1–4 represent mainly shallow marine carbonate environments, and Facies 5–11 consist of slope to marginal basin deposits. Facies 1–4 were observed only in the lower part of the Bac Thuy Formation exposed near the Ky Cung River (KC01, Figs. 1, 3, 6). Facies 11b, which consists of siliciclastic slump beds, dominates the top part of the Lang Son Formation in an exposure at Na Trang village (NT03, Figs. 1, 3). The Smithian–Spathian boundary in the upper Bac Thuy Formation occurs within Facies 8, which is characterized by organic-rich dark gray limestone and mudstone.

4.1. Facies 1: Lenticular, wavy, and thin flat-bedded carbonates (Facies 1a), and intraclastic limestone containing angular flat carbonate pebbles and cobbles (Facies 1b)

4.1.1. Description

Facies 1 is subdivided into two subfacies: lenticular, wavy, and thin flat-bedded carbonates (wackestone, lime mudstone, and dolomite) and organic-rich mudstone layers (Facies 1a, Figs. 6–8) and intraclastic limestone (rudstone and floatstone) containing angular flat carbonate pebbles and cobbles (Facies 1b). Thin carbonate layers and wackestone beds of Facies 1a, which range in thickness from several millimeters to 3 cm, commonly exhibit current ripples and both cross- and parallel lamination indicative of bimodal paleocurrents running in southwest- to southeastward and north- to northeastward directions (Fig. 6). Isolated asymmetrical ripples, 1–2 cm high and 5–15 cm long, are occasionally present in the lenticular beds. Lime mudstone and dolomite layers, 1–5 cm thick, are either structureless or display faint parallel lamination. Pyrite aggregations are common in the mudstone layers (Fig. 8C). The bioclastic limestone (wackestone) commonly contains small bivalves.

Facies 1b consists of intraclastic limestone (rudstone and floatstone) containing angular flat carbonate pebbles and cobbles and is characterized by seriously deformed and reworked components of Facies 1a (Figs. 6–8). The angular intraclasts and cracked marl layers occasionally form small tepee structures 2–7 cm thick (Fig. 8). The intraclastic limestone matrixes consist of poorly sorted mudstone and marl. Cracked carbonate layers and beds are commonly found in Facies 1b as well as in Facies 1a.

Some beds of Facies 1b consist of intraclastic limestone characterized by imbrication and, typically, a clast-supported fabric (Figs. 7, 8). The clasts are flat angular pebbles composed of dolomite and laminated and cracked marl; bioclastic limestone (wackestone) clasts include bivalves. These flat carbonate pebbles commonly fill minor channels approximately 1 m wide and several centimeters to 10 cm deep.

4.1.2. Interpretation

Facies 1a and 1b are interpreted to have been deposited in tidal flat environments, between the supratidal to intertidal zones. Lenticular, wavy and thin flat beds are commonly reported in modern tidal flat deposits (Dalrymple, 1992; Pratt et al., 1992; Chakrabarti, 2005; Van den Berg et al., 2007; Dalrymple, 2010; Davis, 2012; Flemming, 2012). Isolated ripples and bidirectionally cross-laminated wackestones in the lenticular and wavy-bedded carbonates and thin mudstone layers (Facies 1) indicate that these are most likely low-energy tidal current deposits. The wavy-bedded carbonates with parallel lamination may have been deposited by suspension fallout from the tidal currents. Tepee structures are generally formed by desiccation in supratidal and upper intertidal zones in arid to semiarid environments (Wright, 1990; Pratt et al., 1992; Wright and Burchette, 1996; Pratt, 2010). Cracks in the lime mudstone may be desiccation cracks. The intraclastic rudstone and floatstone containing abundant imbricated, flat, angular carbonate pebbles and cobbles are likely derived from desiccation-cracked lime mudstone that was reworked by tidal currents or storm-generated waves. Flat, angular pebbles containing ammonoids characterized by upside-down geopetal structures were likely transported from subtidal or shallow marine environments. Minor tidal channels and creeks were commonly filled by granules, pebbles, and cobbles derived from desiccated carbonate.

Facies		Lithology	Characteristic sedimentary structures, clasts, and fossils	Interpretation		
1a	3-10cm	Lenticular, wavy, and thin flat-bedded carbonates (wackestone, lime mudstone, and dolomite) and mudstone	• Current ripples and cross-lamination indicating bidirectional paleocurrents.	Tidal deposits	Intertidal /supratidal flat	Carbonate platform
1b	5-20cm	Intraclastic rudstone and floatstone containing dolomite clasts (secondarily deformed or reworked deposits of facies 1)	• Tepee structures and desiccation cracks. • Imbrications and flat pebbles and cobbles containing upside-down geopetal structures.			
2	0.4-0.8m	Intraclastic, oolitic, and bioclastic limestone (rudstone and floatstone)	• Cross-stratification, with mud drapes and reactivation surfaces. • Poorly preserved bivalve shells.	Tidal bundles	Subtidal /intertidal flat	
3	1-60cm	Alternating limestone (bioclastic, oolitic, and intraclastic floatstone and wackestone) and marl (wackestone and lime mudstone)	(Limestone) • Normal grading and structureless. • Abundant well-preserved marine mollusks. (Marl) • Weak lamination.	Subtidal flat to wave-influenced shallow marine deposits		
4	5-60cm	Intraclastic limestone (rudstone)	• Normal grading and structureless. • Poorly preserved molluscan shells.	Transgressive lag deposits		
5	0.2-5m	Limestone breccia (intraclastic floatstone and rudstone)	• Matrix- or clast-supported. • Structureless (chaotic). • Large intraclastic limestone clasts and slump beds.	Debris flow deposits		Slope to marginal basin plain
6	1-4m	Alternating siliciclastic sandstone and mudstone	(Sandstone) • Normal grading, weakly parallel lamination, and climbing ripples, or structureless. (Mudstone) • Weak parallel lamination and weak bioturbation, or structureless.	Concentrated density flow to turbidity flow deposits Hemipelagic siliciclastic deposits		
7	0.3-2m	Alternating limestone (bioclastic and intraclastic floatstone and rudstone) and marl (wackestone and lime mudstone)	(Limestone) • Normally graded shell concentrations, structureless, with ammonoid imbrication. • Abundant molluscan fossils, microfossils, and intraclastic marl clasts (rip-up clasts). (Marl) • Weak bioturbation and structureless. • Common molluscan fossils and microfossils.	Concentrated density flow deposits Hemipelagic calcareous deposits		
8	0.4-3m	Organic-rich dark gray limestone (wackestone) and mudstone containing marl layers	(Limestone) • Parallel lamination and cross-lamination, or structureless. • Common molluscan fossils, and microfossils. (Mudstone) • Weak parallel lamination, or structureless. • Common microfossils and calcareous nodules.	Turbidity flow deposits Hemipelagic siliciclastic deposits		
9	0.1-5m	Bedded marl (wackestone and lime mudstone) containing mudstone layers	• Weak parallel lamination and weak bioturbation, or structureless. • Common microfossils and rare bivalves.	Hemipelagic calcareous deposits		
10	0.1-35m	Thick mudstone intercalated by sandstone and wackestone layers	(Mudstone) • Weak parallel lamination and weak bioturbation, or structureless. (Sandstone) • Cross-lamination and current ripple lamination.	Hemipelagic siliciclastic deposits Turbidity flow deposits		
11a	0.3-6m	Secondarily deformed marl beds	• Folded and deformed beds.	Slump deposits originating from hemipelagic calcareous deposits (Facies 9)		
11b	5-12m	Secondarily deformed alternating siliciclastic sandstone and mudstone		Slump deposits originating from shelf deposits in the Lang Son Fm.		

Fig. 5. Sedimentary facies and depositional environments.

4.2. Facies 2: cross-stratified limestone containing mud drapes and reactivation surfaces

4.2.1. Description

Facies 2 is a poorly sorted cross-stratified limestone bed (intraclastic rudstone, floatstone, and packstone) 30–50 cm thick (Figs. 7, 8). It commonly contains small ooids, poorly preserved bivalve shells, and abundant intraclastic limestone granules and pebbles. The cross-stratification is internally composed of tabular- to wedge-shaped sets of tangential to angular foresets in medium- to coarse-grained deposits. These foresets are commonly overlain by mud drapes 2–15 mm thick or intraclastic mudstone granules (mudstone flakes) (Figs. 7, 8). The foresets dip south- and southwestward at inclinations of up to 30°. Reactivation surfaces are occasionally present in the upper part of the cross-bedding. Facies 2 sometimes overlies minor channel-fill deposits and is associated with Facies 1.

4.2.2. Interpretation

Facies 2 reflects tidal influences and is interpreted to represent intertidal to subtidal calcareous sand-flat environments. Cross-bedded limestone with mud drapes and reactivation surfaces is a characteristic internal structure of tidal dunes in intertidal to subtidal zones (Dalrymple, 1992, 2010). Generally, migration of tidal sand bars is controlled primarily by ebb and flood cycles (Boersma and Terwindt, 1981; Yang and Nio, 1985; Friedman and Chakraborty, 2006; Dalrymple and Choi, 2007), and mud drapes accumulate on the foresets and bottom sets during the slackwater stages that follow the ebb and flood periods. Reactivation (truncation) surfaces are generally formed during reverse flow. The cross-bedded limestone of Facies 2 represents simple small tidal sandbars (tidal dunes). Most of the poorly preserved shallow marine bivalve shells and fragments of ooids in Facies 2 appear to have been transported and reworked by storm and strong tidal currents.

4.3. Facies 3: Alternating bioclastic, oolitic, and intraclastic limestone (floatstone and wackestone) and marl (wackestone and lime mudstone)

4.3.1. Description

Facies 3 is dominated by bioclastic, oolitic, and intraclastic limestone (floatstone and wackestone) (Figs. 9, 10). The limestone beds are

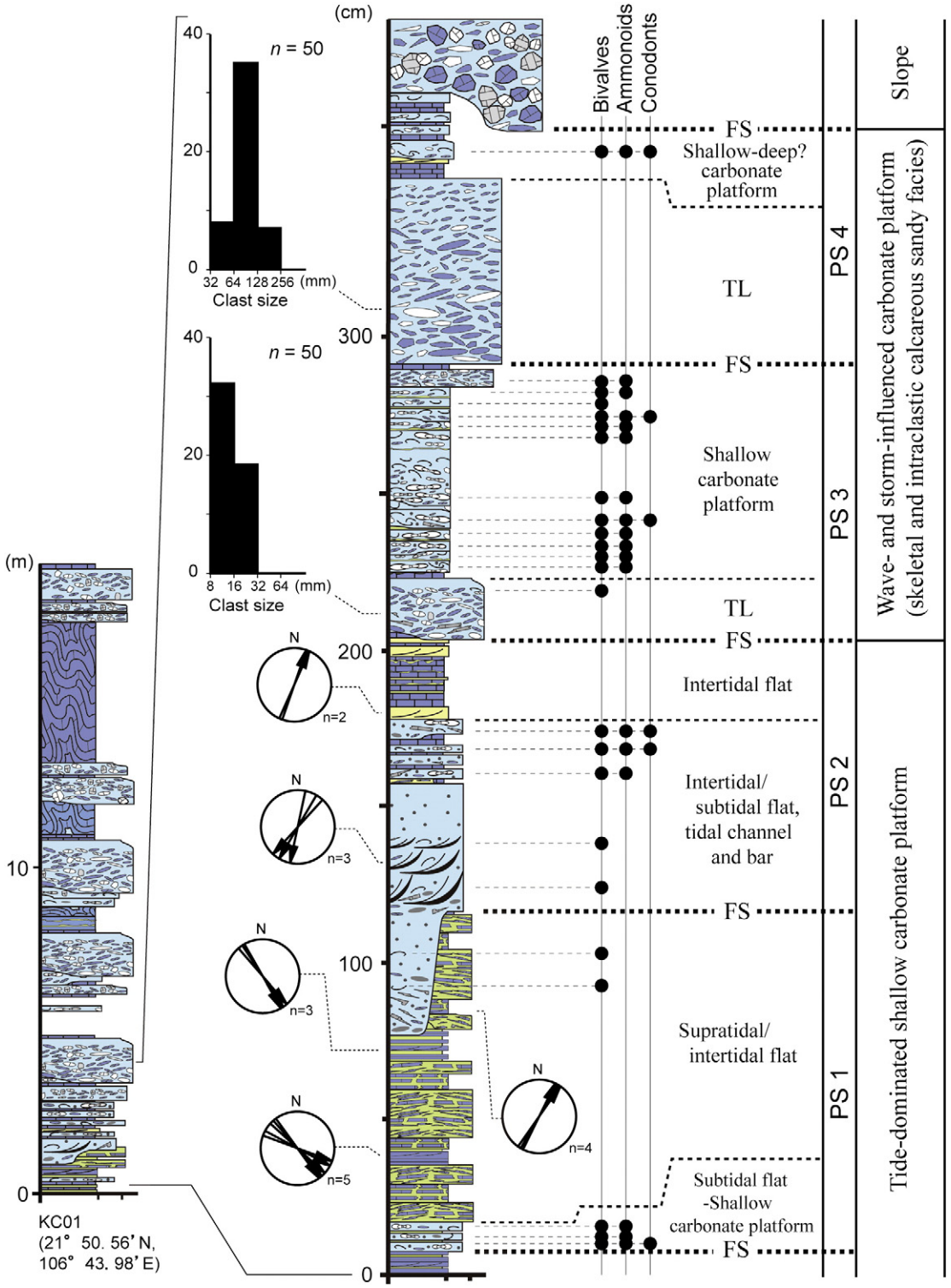

Fig. 6. Detailed stratigraphic column of the lower part of the Bac Thuy Formation (section KC01). Tide-dominated shallow carbonate platform deposits in the bottom of the sequence change upwards into wave- and storm-influenced carbonates. The deepening-upward sequence of fossiliferous shallow marine carbonates is divided into four parasequences (PS1–PS4), which are overlain by slope deposits consisting of limestone breccias. The tidal deposits are characterized by bimodal paleocurrents running in southwest- to southeastward and north- to northeastward directions. Histograms of gravel-sized sediment diameters show that the transgressive lag deposits of PS4 are coarser than those of PS3.

2–5 cm thick and are characterized by sharp, erosive basal surfaces; they are overlain by thin layers of marl (lime mudstone and wackestone). Concentric ooids with diameters of 2–5 mm are commonly replaced by sparry calcite. Fragments of ooids and composite ooids are abundant. The bioclasts consist mainly of small shallow marine bivalves, ammonoids (e.g., *Owenites*), and conodonts (e.g., *Neospathodus waageni* (Sweet) [i.e., *Novispathodus waageni* (Sweet) of Goudemand et al., 2012]). The bivalves are commonly disarticulated. The ammonoids are 1–5 cm in diameter and some ammonoid chambers form upside-down geopetal structures (Fig. 10D). Subangular to subrounded granule-sized intraclasts and peloids are common. The bioclastic and intraclastic limestones occasionally display normal grading and symmetrical

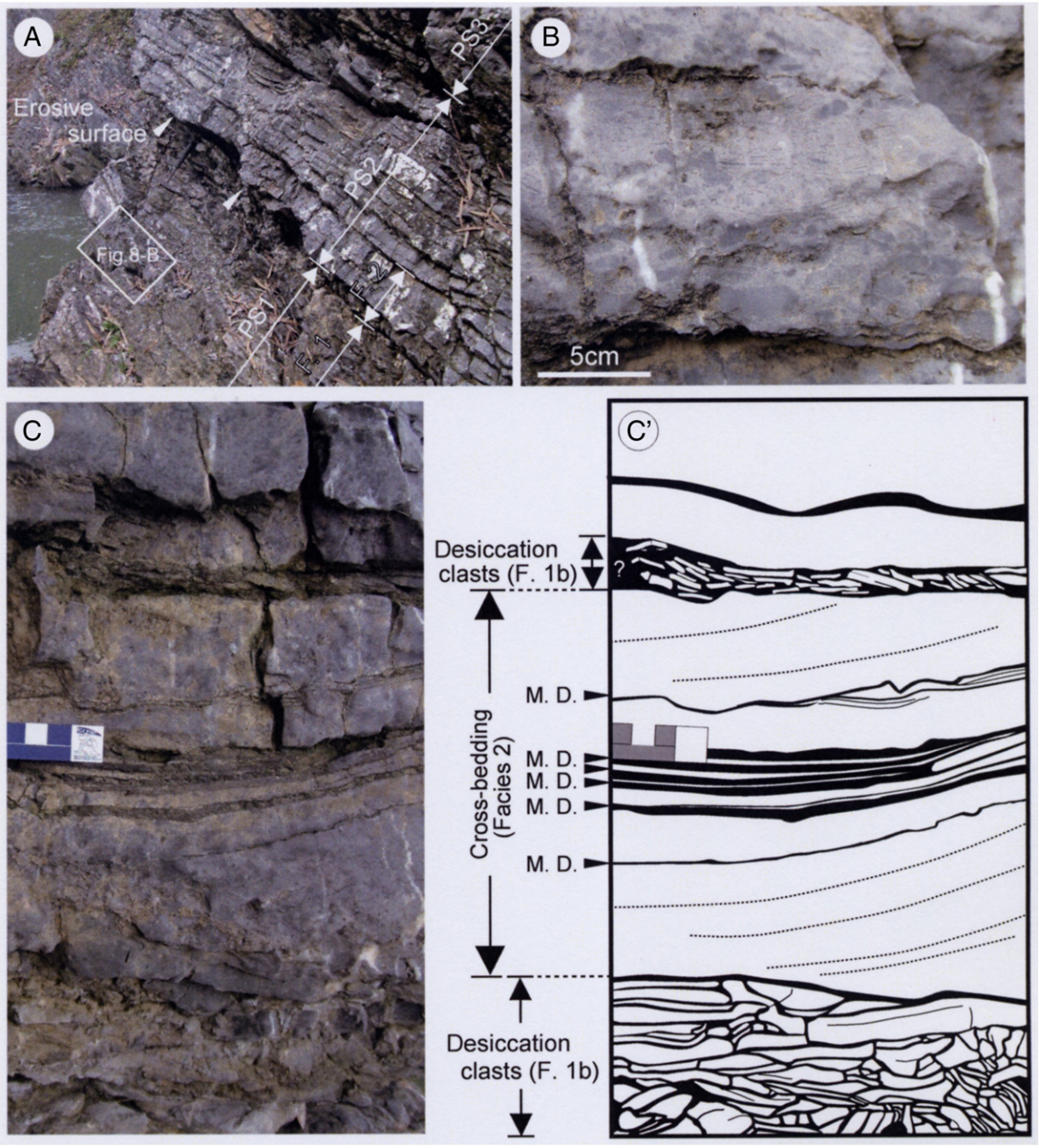

Fig. 7. Shallow marine carbonate lithofacies in the succession in section KC01. F. = Facies. (A) Outcrop view of parasequences PS1–PS3. Arrows indicate the characteristic erosive marine flooding surface between the supratidal/intertidal flat deposits of Facies 1 and the intertidal/subtidal flat carbonates of Facies 2. (B) Bioclastic, oolitic, and intraclastic limestone (Facies 3, PS2). (C) Supratidal/intertidal flat deposits (Facies 1) and tidal bar deposits (Facies 2) in PS2 with mud drapes (M.D.). Facies 1b is composed of imbricated flat pebble and cobble intraclasts and contains tepee structures and desiccation cracks. (C′) Diagram of the section shown in (C).

wave ripples. In cross section, thin disarticulated bivalve shells in some bioclastic layers exhibit an edgewise arrangement (i.e., flat shells are perpendicular to the bedding; Kidwell et al., 1986) (Fig. 10A). The overlying thin lime mudstone and wackestone layers are homogeneous or contain weak lamination and small burrows.

4.3.2. Interpretation

Facies 3, which is associated with the tidal flat deposits of Facies 1 and 2, is characterized by common marine mollusks such as ammonoids, bivalves, and conodonts. Ooids are generated in high-energy shoals (Tucker and Wright, 1990). Normally graded beds consisting mainly of bioclasts, ooids, and intraclasts are commonly reported in storm deposits in shelf and carbonate platform environments (Tucker and Wright, 1990; Tucker, 1991; Johnson and Boldwin, 1996). Symmetrical ripples are formed by wave-generated oscillatory flows. Edgewise shell frameworks generally reflect the influence of strong wave currents (Kidwell et al., 1986). Therefore, Facies 3 may represent the deposition of skeletal and ooid calcareous sand bodies associated with subtidal flat or storm-wave-influenced shallow marine environments.

4.4. Facies 4: structureless intraclastic limestone (rudstone)

4.4.1. Description

Facies 4 is a structureless intraclastic rudstone, 5–60 cm thick, composed of clast-supported subangular to subrounded flat pebbles and cobbles of lime mudstone. Two conspicuous beds are present in

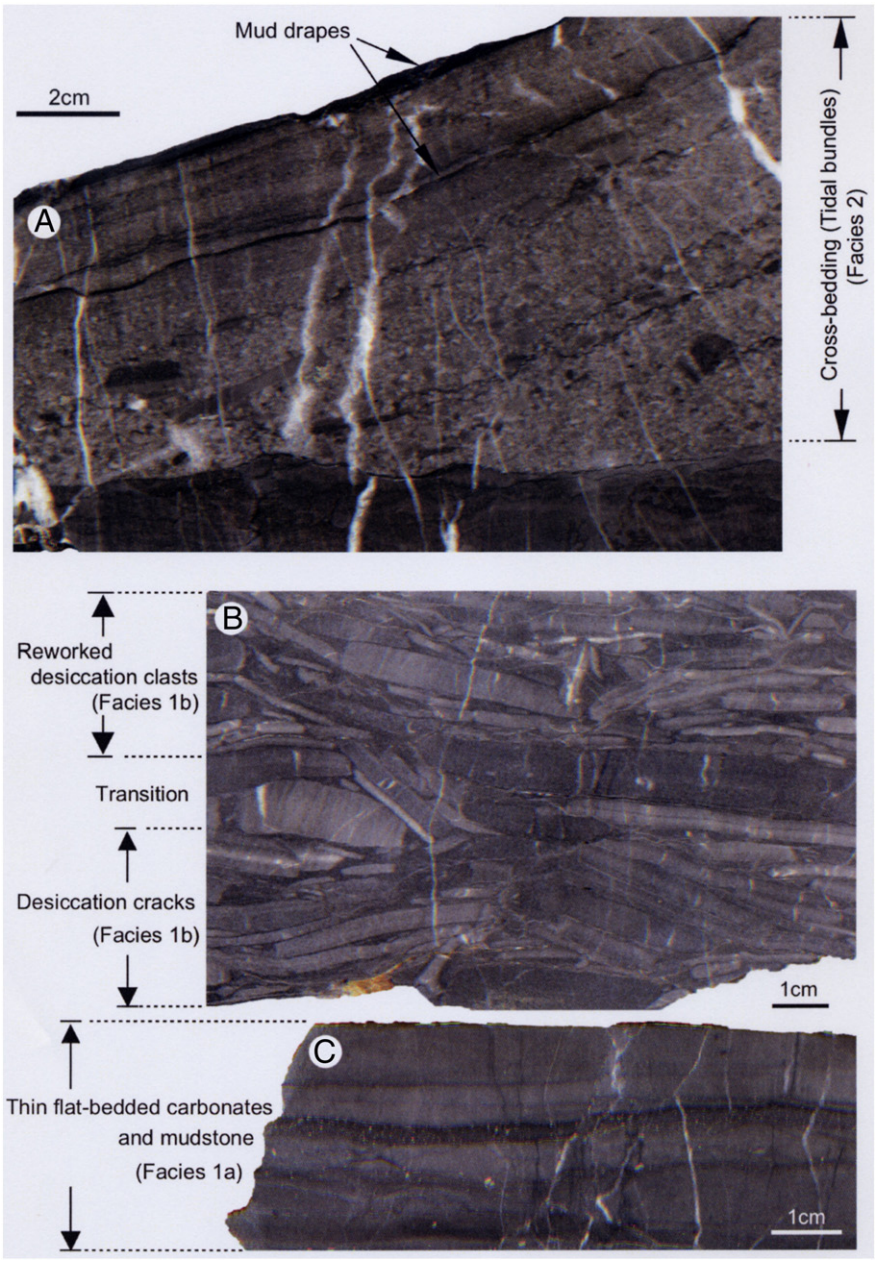

Fig. 8. Vertical cross sections of slabs from section KC01 showing tidal deposits. (A) Cross-stratified intraclastic and oolitic limestone with several mud drapes (Facies 2, PS2) and tidal bundle deposits. (B) Intraclastic limestone containing tepee structures and desiccation cracks (Facies 1b, PS1). Note the desiccation-cracked bed covered by reworked desiccation clasts. (C) Thin flat-bedded carbonates and mudstone (Facies 1a, PS1).

the lower part of the sequence in the KC01 section (Figs. 3, 6). The erosive basal surfaces are sharp and wavy. The matrices contain rare, poorly preserved bivalve and ammonoid bioclasts. Occasionally, these limestones exhibit normal grading (Fig. 9B). Although Facies 4 lithologically resembles Facies 1b, the flat pebbles and cobbles in Facies 4 are more rounded and dolomite clasts are rare. Facies 4 overlies shallow marine deposits (e.g., the intertidal deposits of Facies 1) and is overlain by facies formed in relatively deep environments (e.g., the subtidal to wave-influenced shallow marine deposits of Facies 3).

4.4.2. Interpretation

Facies 4 is interpreted as having been deposited in a shallow marine environment because it overlies Facies 2, which is composed of intertidal deposits, or is intercalated within Facies 3, which contains abundant shallow marine mollusks. The intraclasts and poorly preserved bioclasts in this facies are inferred to have resulted mainly from powerful erosion generated by storm and wave currents on major marine flooding surfaces (Fig. 6). Storm deposits (tempestites) commonly contain flat, angular to subrounded intraclasts and display normal grading (Aigner, 1982; Tucker and Wright, 1990). The intraclastic limestone of Facies 4 may represent transgressive lag deposits, and its basal erosive surface may therefore represent a major marine flooding surface.

4.5. Facies 5: limestone breccia (intraclast floatstone–rudstone)

4.5.1. Description

Facies 5, which is 0.1–4 m thick, consists dominantly of thick, structureless, clast- or matrix-supported limestone breccia containing intraformational tabular and spherical limestone pebbles, cobbles, and boulders. These rocks characteristically form calcarenitic bodies with channel-like geometries (Figs. 11, 12). The matrix consists primarily of wackestone and lime mudstone. The subrounded to rounded pebbles

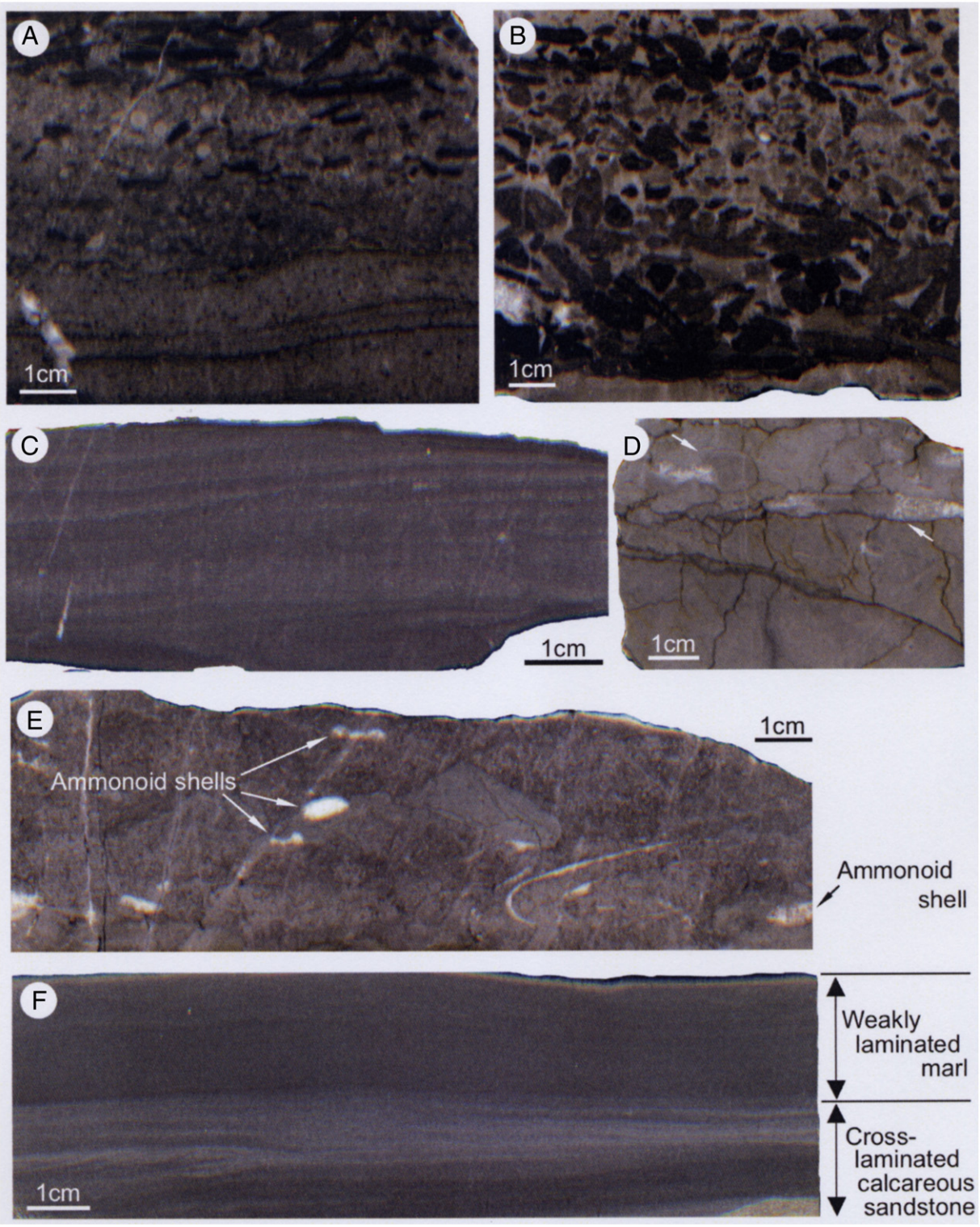

Fig. 9. Vertical cross sections of limestone slabs. (A) Intraclastic, oolitic, and bioclastic limestone (Facies 3, PS3, section KC01). (B) Intraclastic limestone showing normal grading (Facies 3, PS3, section KC01). (C) Low-angle cross-stratified limestone (Facies 3, PS2, section KC01). (D) Bioclastic limestone containing ammonoid (arrows) and bivalve shells (Facies 7, section PK01). The ammonoid shells exhibit geopetal structures. (E) Bioclastic and intraclastic limestone containing ammonoid shells (arrows) (Facies 7, section KC02). (F) Cross-laminated calcareous sandstone layer overlain by weakly parallel-laminated marl (Facies 10, section KC02) indicating a low-density turbidite.

and cobbles are derived from bioclastic and intraclastic wackestone and floatstone (Facies 3, 7) and lime mudstone from underlying beds or from the shallow marine oolitic limestones of Facies 3. Outsized limestone boulders ranging from several tens of centimeters to approximately 5 m in diameter are often present in the middle and upper parts of thick limestone breccia beds. Occasionally, the breccia includes slump-folded and strongly deformed limestone beds containing bioclasts and intraclasts (Fig. 11B).

Facies 5 also contains coarse calcareous sandstone beds with limestone granules and small pebbles. The sandstone is characterized by normal and inverse grading, parallel lamination, and climbing-ripple lamination (Figs. 13, 14). Normally graded sandstone beds contain

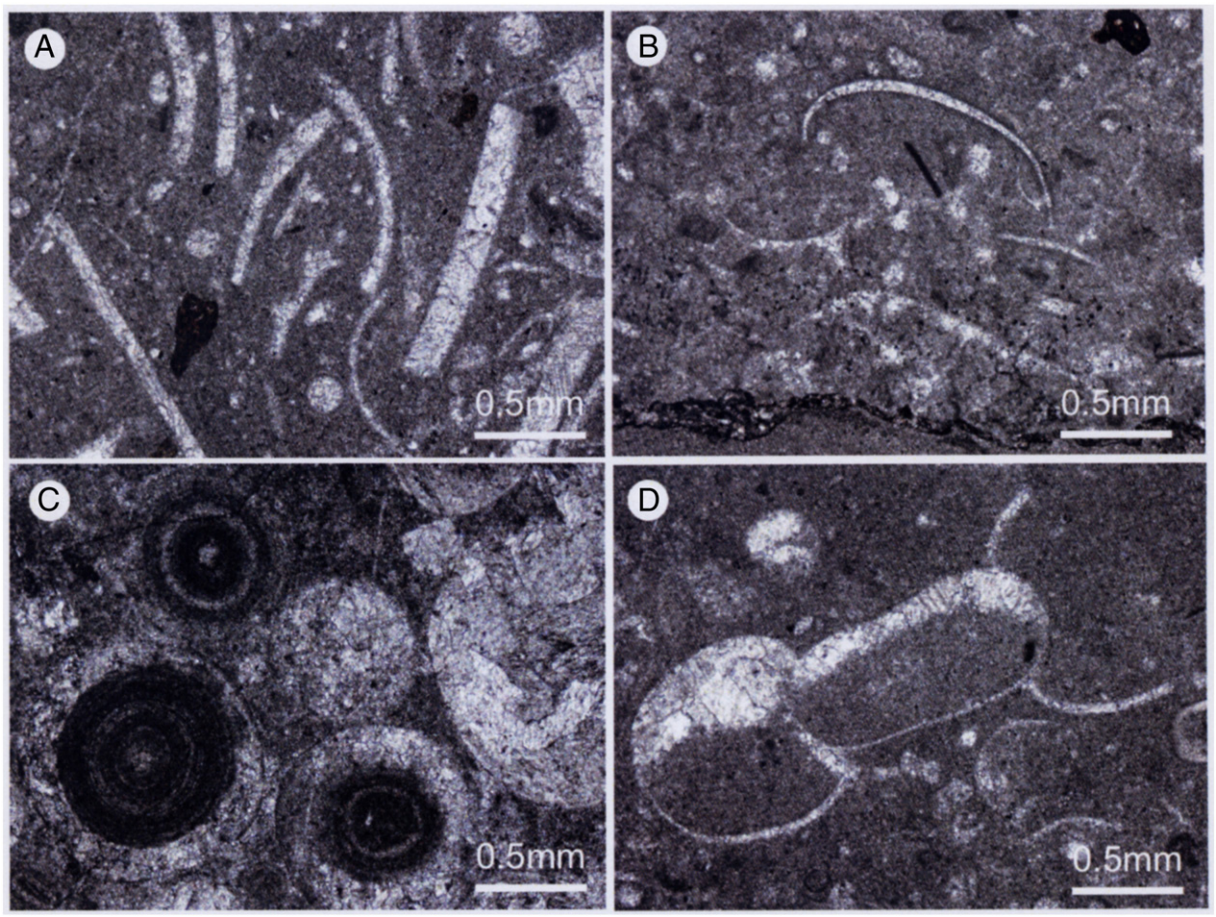

Fig. 10. Photomicrographs of vertical thin sections showing the characteristics of facies exposed in section KC01. (A) Bioclastic and intraclastic wackestone (Facies 3, PS3). Thin bivalve shells are arranged edgewise and perpendicular to the bedding. This edgewise shell framework was formed by strong wave currents. (B) Bioclastic and intraclastic wackestone (Facies 3, PS3). (C) Oolitic wackestone (Facies 3, PS2). (D) Bioclastic wackestone containing juvenile ammonoids (Facies 3, PS3). One ammonoid shell displays a geopetal structure.

granule- to pebble-sized intraformational (rip-up) mudstone clasts at the base. Occasionally, basal flame structures are present (Fig. 13B). Current-ripple and climbing-ripple laminations indicate primarily eastward to northeastward paleocurrent directions at KC02 and NT01 (Fig. 3). The overlying mudstone is characterized by lamination and weak bioturbation (Fig. 14C) and commonly bears radiolarians and thin-shelled bivalves.

At NT02, Facies 5 is characterized by channel-like bodies of calcarenite that are up to 8 m thick and more than 30 m wide (Figs. 3, 12A) with erosive bases incised up to several meters into the underlying mudstones of Facies 9–11. These bodies are scattered unsystematically within the hemipelagic mudstones of Facies 10 (Fig. 3). Facies 5 overlies and is also usually capped by Facies 7–11a. Amalgamated deposits are commonly observed in Facies 5.

4.5.2. Interpretation

Facies 5 is interpreted as debris flow deposits filling erosional channels formed by mass-transport processes (Posamentier and Kolla, 2003; Posamentier and Walker, 2006) with intercalated beds of concentrated density flow deposits (sensu Mulder and Alexander, 2001). The limestone breccias were generated by the collapse of early lithified carbonates that were derived mostly from the carbonate platform margin. The structureless clast- or matrix-supported textures of the thick limestone breccia (debrite) are indicative of hyperconcentrated density flow or debris flow deposits (Lowe, 1979; Stow et al., 1996; Mulder and Alexander, 2001). Matrix-supported gravels are interpreted to have been supported by the yield strength of the interstitial mud in debris flows (Johnson, 1970). The tabular cobble- to boulder-sized intraclasts suggest erosion of semiconsolidated interbedded limestone and lime mudstone at the basal surface by highly erosive sediment gravity flows (Postma et al., 1988); deformed sedimentary blocks exhibiting slump folding in the limestone breccia may have been produced by unstable channel walls. These outsized clasts suggest the presence of plug flows in the upper part of a high-concentration sediment gravity flow (Lowe, 1979, 1982; Postma et al., 1988).

The erosive channel surfaces indicate frequent gravity flow episodes of highly concentrated sediments that produced incisions 2–5 m in depth. Amalgamated thick limestone breccia suggests repeated episodic depositional events. Isolated or discontinuous tongued channel-fill debris flow deposits are typically present in marginal basin plain environments (Stow et al., 1996; Posamentier and Kolla, 2003; Posamentier and Walker, 2006; Payros et al., 2007). Modern examples of debris flow deposits filling low-sinuosity channels are common in slope to basin-floor settings (Posamentier and Kolla, 2003; Playton et al., 2010). In the Eocene Anotz Formation in the western South Pyrenean foreland basin, Europe, Payros et al. (2007) reported limestone breccia filling channels of various sizes in calciclastic submarine slope and lobe deposits. In Santa Agueda and Poza Rica, Mexico, Janson et al. (2011) described channels in the Cretaceous platform slope ranging from 300 to 600 m in width and from 60 to 160 m in depth. The channels in the Bac Thuy Formation are much smaller than these recent and fossil channels, and they are very shallow and small compared with modern submarine canyons reported by Mullins and Cook (1986) and Tucker and Wright (1990). For example, the entire complex of minor and amalgamated channels in the Bac Thuy Formation is only 8 m thick and just over 30 m wide, whereas in the Little Bahama Bank,

Fig. 11. Slope deposits in the lithofacies succession at section KC02. (A) Outcrop view of the succession from slope to marginal basin deposits, including the Smithian–Spathian boundary. A thick limestone breccia containing outsized intraclasts can be clearly observed (Facies 5). (B) Limestone breccia containing slumped beds (Facies 5). (C) Matrix-supported limestone breccia (Facies 5). (D) Clast-supported limestone breccia containing oolitic and bioclastic wackestone intraclasts (Facies 5). (E) Oolitic wackestone cobble-sized intraclast in limestone breccia.

gullies and V- or U-shaped canyons exhibit 20–150 m of topographic relief and can be up to 3 km wide (Mullins and Cook, 1986). Thus, the debris flow deposits of Facies 5 are interpreted as shallow channel fills in the surfaces of slump and hemipelagic deposits. In this area, debris flow channels are not associated with thick rhythmic or sheet-like turbidity flow deposits. Furthermore, concentrated density flow deposits are rarely present in this carbonate facies. Most sand-sized sediments were likely transported past the slope environment where these channels existed, whereas fine-grained carbonates (marls) accumulated within the channels and interchannels as a result of sediment fallout from suspension.

The normal- and inverse-graded gravelly calcareous sandstone was likely deposited by a concentrated density flow (Lowe, 1979; Mulder and Alexander, 2001). Inverse-graded layers in the basal parts of the

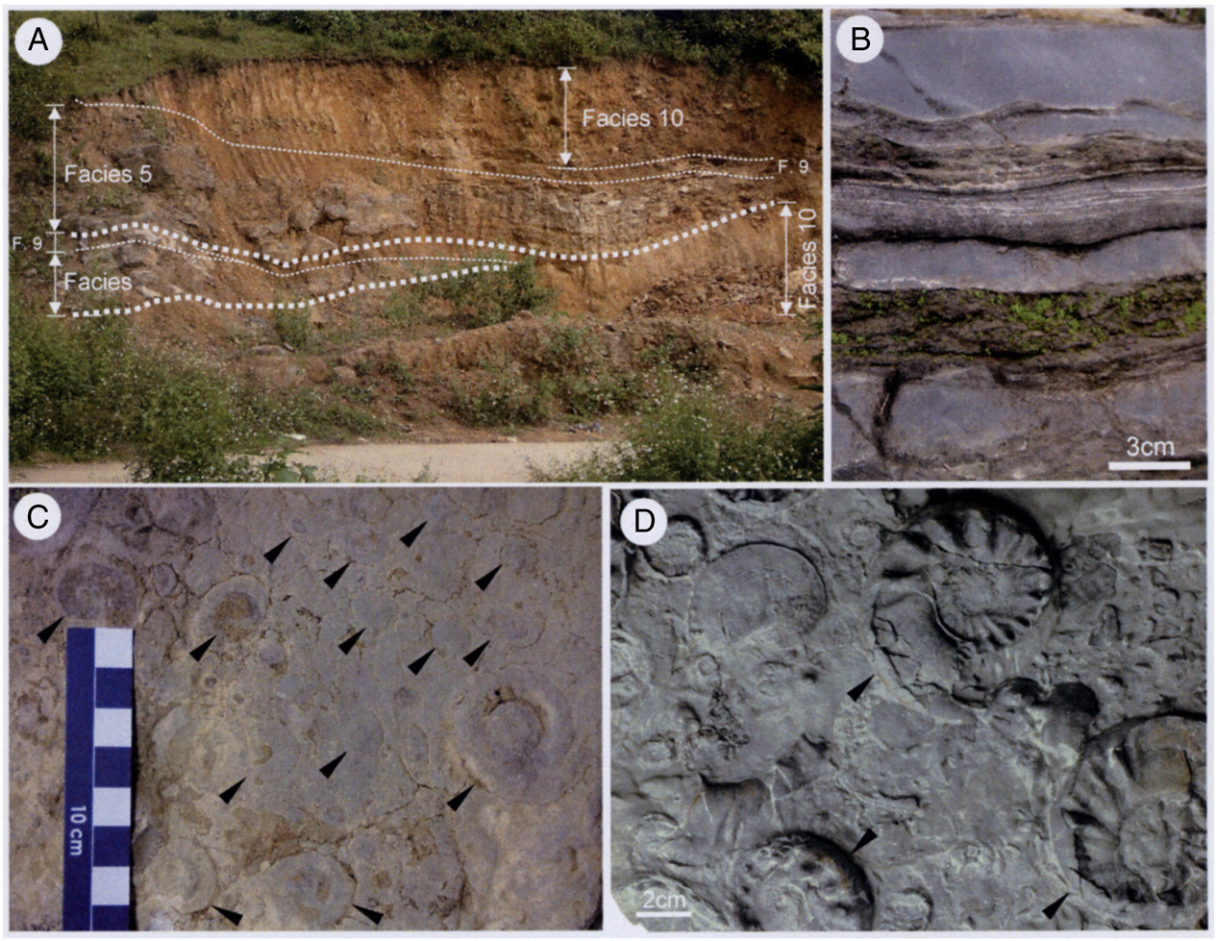

Fig. 12. Lithofacies of slope deposits and modes of occurrence of ammonoids. (A) Outcrop view of isolated channel-filling limestone breccia (Facies 5) in hemipelagic mudstone (Facies 10, section NT02). (B) Thin-bedded hemipelagic limestone and marl (Facies 9, section KC02). (C) Bioclastic limestone with abundant ammonoids (arrows) and a shell-supported fabric (Facies 7, plane view, section PK01). (D) Well-preserved Spathian *Tirolites* ammonoids (arrows) in a low-density turbidite layer (Facies 10, plane view, section KC02).

beds are typical features of coarse-grained sediment gravity-flow deposits, although their origin remains controversial (Hiscott, 1994; Sohn, 1997). This basal inverse-grading structure corresponds to Lowe's S2 division (Lowe, 1982). The graded bedding and climbing ripples indicate that these deposits were not formed by instantaneous freezing of a high-concentration sediment flow; rather, they imply continuous deposition during turbulent flow (Mulder and Alexander, 2001). However, the large grains in this facies suggest that sediment in the flow may have been highly concentrated enough to support particles by a process such as hindered settling. Sohn et al. (2002) reported that debris flows commonly change to concentrated density flows in submarine environments. The close stratigraphic relationship between debris-flow deposits and concentrated density flow deposits in this facies suggests the occurrence of such flow transformations (Fig. 3).

4.6. Facies 6: alternating sandstone and mudstone

4.6.1. Description

Facies 6 is characterized by alternating beds of greenish gray or light gray to gray sandstone (3–60 cm thick) and mudstone (2–70 cm thick). The very fine to medium-grained sandstone beds have a sheet-like geometry with a sharp erosive base (Fig. 13F). The basal to middle parts of the sandstone beds are generally structureless, but parallel and convolute lamination and climbing ripples are commonly observed at their tops. The sandstones are covered by structureless mudstone containing rare small, very thin shells of *Bositra* (so-called *Posidonia*). Facies 6 overlies Facies 8 or 10 and is overlain by volcanic rocks of the Khon Lang Formation in the Ky Cung River, Na Trang, and Pac Khanh sections.

4.6.2. Interpretation

The structureless and parallel-laminated sandstones of Facies 6 are equivalent to the thin-bedded turbidites of divisions Ta and Tb, respectively, in the Bouma sequence (Bouma, 1962). The climbing ripples capping the sandstone beds belong to Bouma division Tc. Thus, these sandstones are considered to be classical turbidites (Posamentier and Walker, 2006). A structureless bed (division Ta) overlain by climbing ripples most likely represents deposition during transition from a concentrated flow to a turbidity flow. Climbing-ripples and convolute lamination imply moderately high rates of sediment fallout from suspension (Walker, 1985). The weakly laminated mudstones intercalated in these gravity flow deposits were most likely transported in part by the turbidity flows. Some beds contain radiolarians and articulated paper-shelled bivalves; thus, most of the mudstones are interpreted to be hemipelagic in origin.

4.7. Facies 7: alternating bioclastic and intraclastic limestone (floatstone and rudstone) and marl (wackestone and lime mudstone)

4.7.1. Description

Facies 7 is composed mainly of thin (3–10 cm) beds of light gray bioclastic and intraclastic limestone (floatstone and rudstone) and marl (wackestone and lime mudstone). Bioclastic wackestone and packstone are also commonly present in this facies. The bioclastic

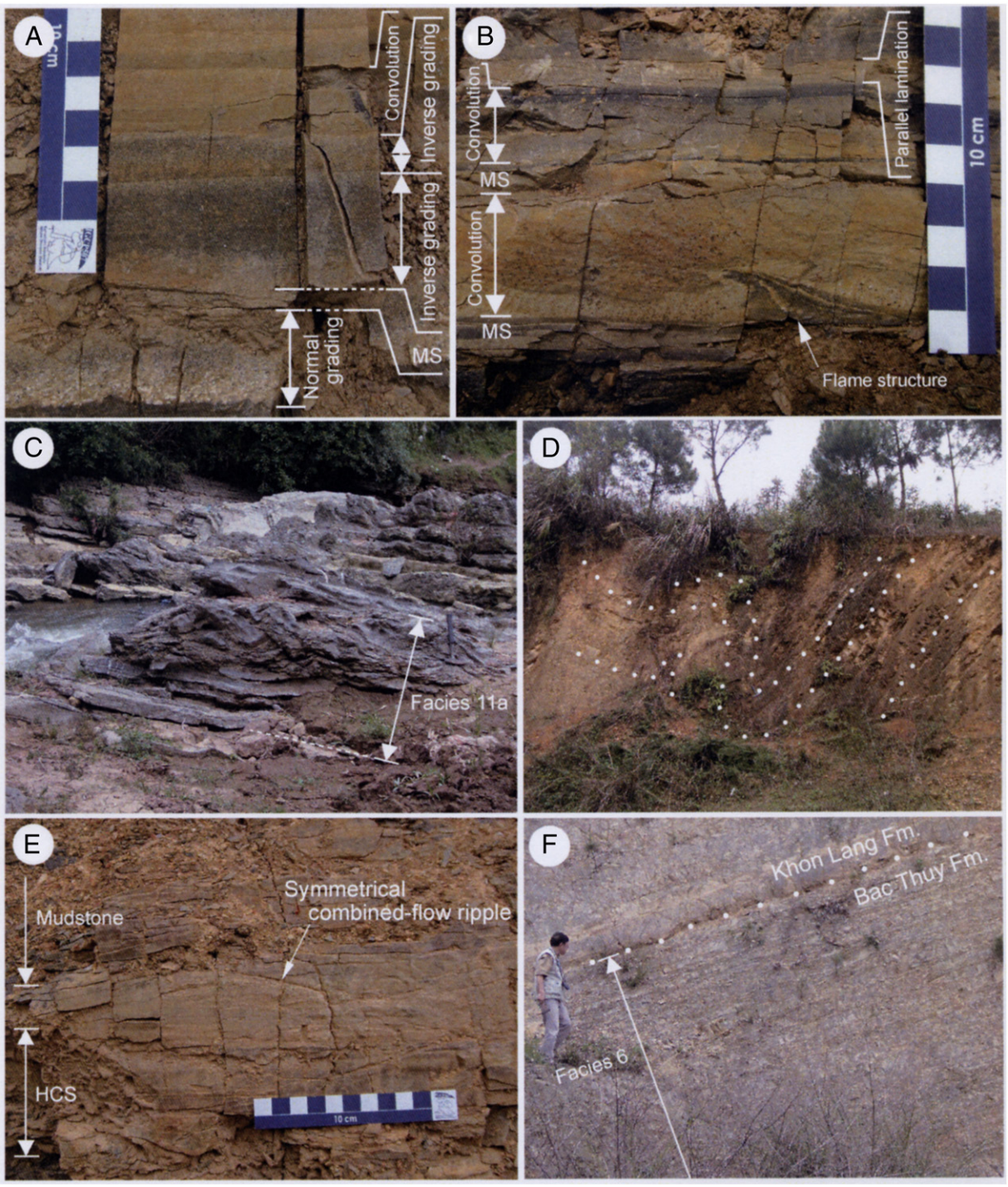

Fig. 13. Outcrops of the upper Lang Son Formation and the Bac Thuy Formation. MS = mudstone. (A) Gravelly and very coarse calcareous sandstone displaying normal and inverse grading in the Bac Thuy Formation (Facies 5, section NT01). These calcareous sandstones are overlain by ripple-laminated and convolute-laminated calcareous sandstones. (B) Alternating convolute- and parallel-laminated calcareous sandstone and mudstone in the Bac Thuy Formation (Facies 5, section NT01). A flame structure can be observed in the basal part of the convolute-laminated sandstone. (C) Secondarily deformed bedded limestone (slump bedding) in the Bac Thuy Formation (Facies 11a, section KC01). (D) Secondarily deformed alternating siliciclastic sandstone and mudstone (slump bedding) in the upper Lang Son Formation (Facies 11a, section NT03). (E) Alternating siliciclastic very fine sandstone and mudstone in the upper Lang Son Formation, Na Trang area. Symmetrical combined-flow ripples overlie hummocky cross-stratified (HCS) sandstone. (F) Alternating siliciclastic very fine to fine sandstone and mudstone near the top of the Bac Thuy Formation (Facies 6, section NT01). Fm. = Formation.

limestones are characterized by sheet-like or concave-upward geometries with erosive bases and flat tops; they contain abundant ammonoids, disarticulated bivalves, shark teeth, conodonts, and poorly preserved shell fragments. The basal layers are characterized by lenticular shell concentrations in a clast-supported fabric, which commonly bear ammonoids 5–15 cm in diameter (Figs. 9, 12). The bioclastic limestones are generally structureless (homogeneous) and occasionally show normal grading and shell imbrications at the tops of the shell concentrations. The ammonoid shells often display geopetal structures. Intraclasts and peloids are also common. The intraclastic limestones contain subrounded tabular and spherical granules and pebbles.

The wackestone and lime mudstone are either massive or display weak parallel lamination. They commonly overlie bioclastic limestone

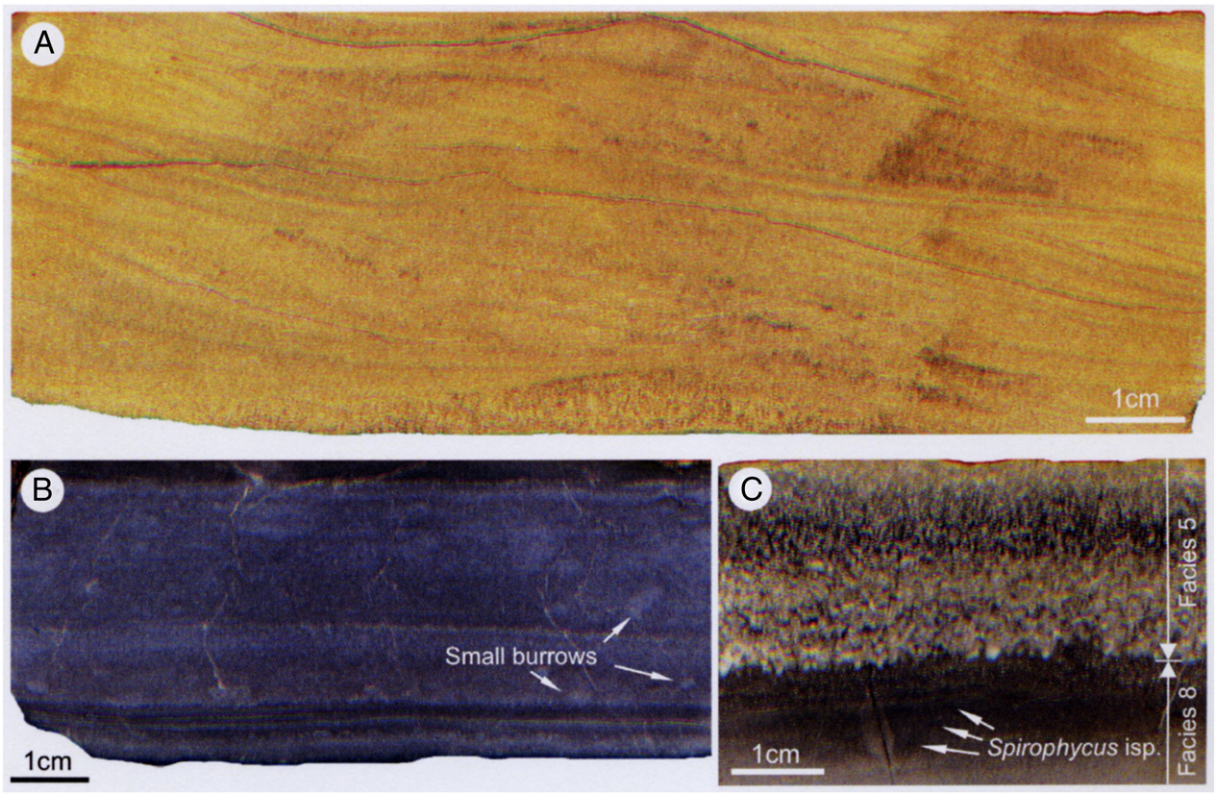

Fig. 14. (A) Alternating very fine siliciclastic sandstone displaying climbing-ripple lamination (Facies 6, section NT01). (B) Laminated organic-rich dark gray limestone containing small burrows (Facies 8, KY02) overlying well-laminated organic-rich black lime mudstone. (C) Calcareous sandstone displaying normal grading (Facies 5) and weakly bioturbated organic-rich black lime mudstone containing tiny *Spirophycus* isp. ichnofossils (Facies 8, section NT01).

beds and contain small burrowers and thin-shelled bivalves. Facies 7 overlies and is overlain by Facies 5 and 9–10.

4.7.2. Interpretation

Facies 7 consists mainly of calciclastics, which are characteristic of concentrated density flow deposits. The erosive basal surfaces indicate frequent gravity flow episodes that produced minor, shallow incisions in the surfaces of the underlying deposits. Abundant shell fragments, normal grading, and erosive basal surfaces suggest that the sediments were transported in concentrated density flows. The structureless beds that dominate this facies imply a relatively high sediment concentration flow in which processes such as synsedimentary liquefaction of basal sediments often occurred (Fig. 9E). The intraclasts and poorly preserved shells most likely represent lag deposits that were agitated and mixed with transported shells. Imbricated ammonoids seem to have been rearranged by the gravity flows. Lenticular shell concentrations infilling minor shallow channels are typical of slope facies, and they have been interpreted as deposits derived from sediment gravity flows (Komatsu et al., 2008). The weakly bioturbated marl is mostly hemipelagic in origin.

4.8. Facies 8: organic-rich dark gray bioclastic limestone (wackestone) and mudstone

4.8.1. Description

Facies 8 is composed of dark gray bioclastic wackestone, which contains radiolarians and mollusk shells, and dark gray mudstone (Figs. 14, 15). The wackestone beds are 3–30 cm thick and exhibit weak parallel and cross-lamination. These characteristics are similar to Facies 6, 7, 9, and 10; however, Facies 8 is distinguished by occasional bioturbation, small pyrite crystals up to 0.6 mm in diameter, aggregates, and high concentrations of organic matter. Very small grazing traces (pascichnia), such as *Spirophycus* isp. and *Phycosiphon* isp., are common in some layers (Fig. 14). The ichnofossil assemblages are characterized by low diversity and moderately high density.

The mudstone contains abundant molluscan fossils, microfossils, and dark gray limestone nodules. The microfossil assemblage is composed mainly of spheroidal radiolarians and ostracods (Fig. 15C, D). Komatsu et al. (2011, 2013) reported a monospecific ammonoid assemblage composed of *X. variocostatus* and a thin-shelled epifaunal bivalve assemblage consisting mainly of well-preserved *Crittendenia* in this facies. Molluscan shells are found in thin lenticular shell concentrations, approximately 1 cm thick and 20–100 cm wide, in the mudstone and in limestone nodules.

The Smithian–Spathian boundary, which is indicated by the first appearance of a species of tirolitid ammonoid, is apparent within Facies 8; it is conspicuous in the upper part of the Bac Thuy Formation in the KC02, BR01, and NT02 sections (Fig. 3). Facies 8 overlies and is overlain by Facies 5 and 10.

4.8.2. Interpretation

Facies 8 is interpreted to represent an anoxic to dysoxic depositional environment. Organic-rich laminated wackestone and mudstone showing no evidence of bioturbation indicates passive activity of benthic organisms. Pyrite aggregates can be generated in anoxic sediments or in stagnant water. Low-diversity, moderately high-density small grazing traces (pascichnia) indicate activity by opportunistic producers (Bromley, 1996). Ekdale and Mason (1988) proposed that pascichnia-dominated trace fossil assemblages form in less oxygenated conditions than domichnia (burrow)-dominated assemblages; therefore, anoxic to dysoxic conditions likely characterized the depositional environment of Facies 8.

The parallel- and cross-laminated wackestone may be a distal turbidite, corresponding to divisions Td and Te in the Bouma sequence. Allochthonous disarticulated bivalves and ammonoid shells

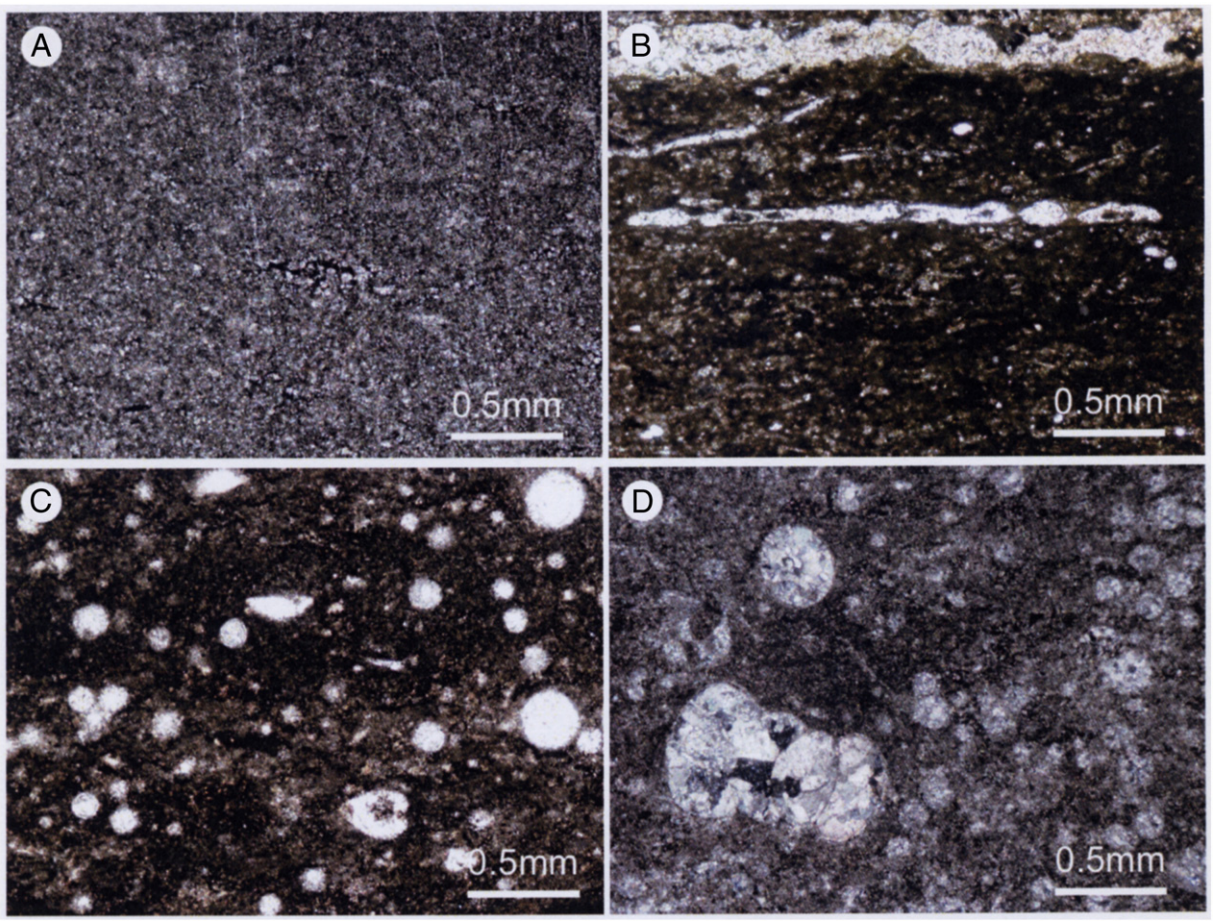

Fig. 15. Photomicrographs of vertical thin sections. (A) Lime mudstone (Facies 9, section KC02). (B) Organic-rich mudstone containing flattened molluscan shells (Facies 8, section NT01). (C) Organic-rich dark gray calcareous nodule containing abundant spheroidal radiolarians and ostracods (Facies 8, section NT01). (D) Dark gray bioclastic wackestone containing juvenile ammonoids and abundant spheroidal radiolarians (Facies 8, section NT01).

were transported by turbidity flows. Maeda and Shigeta (2009) reported that turbulence within turbidity flows causes minimal damage to ammonoid shells during transport; thus, well-preserved ammonoids can be observed in distal turbidites. The mudstone, which contains abundant radiolarians, appears to consist of typical hemipelagic deposits. In the upper part of the Bac Thuy Formation, Facies 8 is associated with the very fine-grained calcareous sandstone of Facies 10, a classical turbidite.

4.9. Facies 9: bedded marl (wackestone and lime mudstone) with mudstone layers

4.9.1. Description

Facies 9 is 1–5 m thick and is characterized by 1- to 20-cm-thick marl beds with intercalated thin layers of calcareous sandy mudstone. Very thin lenticular shell concentrations, up to 2 m wide, are also present in this facies. They are composed mainly of ammonoid and bivalve shells and microfossils such as foraminifers (e.g., *Rectocornuspira* and *Globivalvulina*), radiolarians, conodonts, and ostracods. Poorly preserved shell fragments are abundant in the shell concentrations. The tops of the lime mudstone beds occasionally exhibit weak lamination and contain small two- and three-dimensional burrows 1–2 mm in diameter. Facies 9 is associated with Facies 5, 7, and 10.

4.9.2. Interpretation

The bedded marls of Facies 9 are composed mainly of hemipelagic calciclastics. The thin wackestone, which displays weak lamination and contains bioclasts, was deposited by turbidity flows. The lime mudstone seems to have originated from calcareous mud suspended in turbidity currents. After the passage of the turbidity currents, small benthic organisms burrowed into the sediment surface.

4.10. Facies 10: thick mudstone with intercalated thin sandstone and marl beds

4.10.1. Description

Facies 10, which is more than 5 m thick, is characterized by thick layers of gray and greenish gray mudstone and lime mudstone. The mudstone is weakly laminated and contains small burrows and radiolarians. *Planolites*-like burrows are common. In the upper Bac Thuy Formation, this facies is intercalated by thin beds of lime mudstone and very fine- to fine-grained calcareous sandstone (ca. 1–3 cm thick) containing ammonoids, disarticulated bivalves, and shell hashes in thin lenticular shell concentrations. Thin-shelled epifaunal bivalves such as *Crittendenia*, *Leptochondria*, and *Bositra* are common in the mudstone and in the lenticular shell concentrations in the sandstone, but ammonoids are scarce in the mudstone. The thin sandstone beds are characterized by normal grading and parallel and ripple cross-lamination.

4.10.2. Interpretation

Facies 10 is interpreted as slope to marginal basin plain hemipelagic mudstone deposits. Thin sandstone beds are typical of distal turbidites, equivalent to the upper part of the Bouma sequence (Tc to Te). The thick mudstone seems to have originated as suspension fallout from multiple turbidity flow events. Most of the thin-shelled bivalves and ammonoid

shells in the lenticular shell concentrations were transported to this facies by turbidity flows. The mudstone accumulated from suspension under calm conditions. *Planolites*-like burrows are common in poorly oxygenated deep-sea environments (Bromley, 1996).

4.11. Facies 11: deformed bedded carbonates and siliciclastics

4.11.1. Description

Facies 11 is subdivided into deformed limestone beds (Facies 11a) and alternating beds of deformed siliciclastic sandstone and mudstone (Facies 11b). This facies is composed of heterolithic units of folded and seriously deformed structures (Fig. 13) and is up to 2–15 m thick. The folded and deformed beds of Facies 11a occasionally grade laterally into matrix-supported limestone breccia. The basal portions of Facies 11a are usually chaotic. Almost all of these deformed beds were originally bedded hemipelagic lime mudstone intercalated by thin wackestone and calcareous mudstone layers (Facies 9).

The alternating very fine- to fine-grained siliciclastic sandstone and mudstone layers (Facies 11b), which are deformed into large-scale folds and overturned folds, are found in the upper part of the Lang Son Formation in the Na Trang area. The siliciclastic sandstone is 5–60 cm thick and is characterized by HCS, parallel lamination, wave-ripple lamination, and combined-flow ripples (Fig. 13E).

In the lower Bac Thuy Formation, Facies 11a is mostly embedded within Facies 5, but elsewhere, the thin (0.3–1.5 m thick) deformed beds of Facies 11a commonly underlie Facies 5. Thick mudstone is intercalated by Facies 11b in the upper Lang Son Formation.

4.11.2. Interpretation

These heterolithic units characterized by folds and deformed beds imply slope-induced slumping along an unstable shelf margin. The deformation was caused by shear stress from overriding debris flows, as evidenced by debris flow deposits overlying thin deformed beds.

The slump deposits of Facies 11b, consisting of alternating beds of deformed mudstone and sandstone characterized by HCS, wave ripples, and combined-flow ripples, are typical of shelf environments. The sandstones originally accumulated above the storm-wave base. The alternating beds were most likely deposited in an unstable shelf margin environment above the storm-wave base, and then subsequently slumped onto the slope. In contrast, Facies 11a did not originate as shallow marine deposits but rather resulted from the deformation of Facies 9 (mainly hemipelagic carbonates). Facies 11a does not contain typical shallow marine carbonates (e.g., oolitic, bioclastic, and intraclastic limestones; Facies 3, 4) or tidal deposits (Facies 1, 2). Thus, Facies 11a may have originated in a slope environment.

5. Facies Associations

5.1. Facies Association A (carbonate and siliciclastic shelf deposits)

Facies Association A is composed mainly of tidal deposits (Facies 1, 2), wave-influenced shallow marine carbonates (Facies 3), and transgressive lag deposits (Facies 4). These coastal deposits are approximately 2.5 m thick and are interbedded in the basal Bac Thuy Formation in section KC-01, which is adjacent to a tributary of the Ky Cung River.

The tidal flat deposits are subdivided into supratidal to upper intertidal deposits (Facies 1) and lower intertidal to subtidal deposits (Facies 2). The supratidal to upper intertidal deposits are composed of wavy, lenticular, and thin, flat-bedded carbonates and mudstone intercalated by desiccated deposits and reworked desiccation clasts. Desiccation cracks and tepee structures are key sedimentary structures indicating semi-arid to arid subaerial environments, including upper intertidal and supratidal zones. The wavy, lenticular, and thin flat bedded carbonates with desiccation clasts are composed of dolomite, marl, and mudstone layers and contain bidirectional paleocurrent indicators that were likely generated by tidal currents. These deposits are intercalated by lower intertidal to subtidal deposits consisting of oolitic limestone and tidal sandbar carbonates (Facies 2) with mud drapes and reactivation surfaces.

The basal carbonate facies of the Bac Thuy Formation changes laterally into the upper part of the Induan to lower Olenekian Lang Son Formation, which consists of siliciclastic slump deposits and storm- and wave-dominated siliciclastic shelf deposits (Figs. 2, 3; Komatsu and Dang, 2007). During the early Olenekian, the siliciclastic shelf environment likely evolved into a tide- and wave-influenced mixed siliciclastic and carbonate shelf environment. In South China, Lower Triassic shallow marine deposits are generally composed of carbonates (Lehrmann et al., 1998, 2001, 2003, 2007b; Galfetti et al., 2008). In the Induan to early Olenekian Chongzuo-Pingguo platform – an isolated platform in southwestern Guangxi Province (adjacent to Lang Son Province), Vietnam – the tidal flat facies consists of cross-bedded grainstone and flaser to lenticular beds with mud drapes and desiccation cracks (Lehrmann et al., 2007a,b).

In the Bac Thuy Formation, the tidal deposits are covered by several beds of shallow marine carbonates characterized by wave ripples and abundant ammonoids, bivalves, conodonts, and rounded clasts (Facies 3, 4). The basal parts of these shallow marine carbonates are transgressive lag deposits (Facies 4). They are approximately 20–50 cm thick and dominated by intraclastic limestone containing fine pebbles and cobbles (Fig. 6). Sediments on the shallow sea bottom were likely reworked and agitated by strong, recurring storm- and wave-generated currents during periods of rapid transgression.

5.2. Facies Association B (slope deposits)

Facies Association B is characterized by slump and debris-flow deposits (Facies 5, 11) and coarse-grained gravity-flow deposits that fill straight channels (Facies 7) incised in hemipelagic sediments (Facies 9, 10). This Facies Association can be interpreted as having been deposited in a submarine slope environment with small gullies.

Slump and debris flow deposits intercalating hemipelagic sediments are characteristic of modern submarine slopes (Stow et al., 1996; Hodgson and Flint, 2005). In particular, slumps commonly occur on unstable slopes with low gradients (Stow et al., 1996). In the carbonate slope facies, debris flow deposits containing limestone boulders and oolitic limestone pebbles likely reflect episodic events initiated by the collapse of platform margin sediments. Cohesive debris flow deposits can also occur distally to a region of submarine slumping when the slump is highly mobile (Prior et al., 1982). Other indicators of a slope succession are channel-fill limestone breccias, slump scars, slides, slumps, and hemipelagic deposits (Mullins and Cook, 1986; Walker, 1992; Hodgson and Flint, 2005; Payros et al., 2007; Arnott, 2010).

We divided Facies Association B into Facies Associations B-1, -2, and -3 on the basis of the composition of the deposits. Facies Association B-1, which is predominantly composed of carbonates, consists mainly of Facies 5 (channel-fill limestone breccia) and Facies 11a (carbonate slump deposits); it is over 14 m thick in the lower Bac Thuy Formation in the Ky Cung River section (KC-01). Facies 7 (alternating bioclastic and intraclastic limestone and marl) and Facies 9 (hemipelagic lime mudstone beds containing mudstone layers) are occasionally embedded in this Facies Association. Facies Association B-2, which is composed of siliciclastics, is dominated by Facies 10 (thick hemipelagic mudstone) and Facies 11b (siliciclastic slump deposits) in the upper Lang Son Formation in the Na Trang area (NT-02, NT-03). Facies Association B-3 is composed of the thick siliciclastic deposits of Facies 10 and the thick carbonate complexes of Facies 5 and 9.

The limestone breccias of Facies Association B-1 were generated by the collapse of lithified carbonate platform margins. The bioclastic and intraclastic limestones of Facies 7 were derived from unlithified and early lithified shelf carbonates; the coarse bioclasts and intraclasts were transported by concentrated density flows. The slump masses of Facies Association B-2 mostly likely originated from unlithified siliciclastic shelf deposits. In the slump deposits, weakly deformed sandstone beds commonly contain HCS and wave and combined-flow ripples. These deformed, alternating beds of wave- and storm-influenced sandstone and mudstone likely represent unstable siliciclastic shelf margin deposits.

5.3. Facies Association C (marginal basin plain deposits)

Facies Association C consists of hemipelagic deposits (Facies 8–10) and sheet-like gravity flow deposits (Facies 6), which are interpreted altogether as marginal basin plain deposits. The lower part of this Facies Association is characterized by calcareous gravelly sandstone (Facies 5), hemipelagic deposits (Facies 9, 10), and organic-rich dark gray limestone and mudstone (Facies 8). Siliciclastic and lime mud were presumably transported from a shallow sea environment and numerous planktonic microfossils (mainly radiolarians) progressively accumulated from the suspended load. The upper part of the Facies Association is dominated by fine-grained hemipelagic deposits associated with Facies 9 (bedded marl) and Facies 10 (thick hemipelagic mudstone). Isolated, thin (approximately 1 m thick) channel-fill limestone bodies (Facies 5) are common in the hemipelagic mudstone. These minor channels may represent the distal ends of larger channels and canyons. Thin turbidites composed of very fine sandstone most likely represent sediments spilled from channels or accumulated at the distal ends of minor channels. Several sets of classical turbidites (Facies 6) seem to have accumulated in frontal splay environments in the marginal basin plain. Frontal splay deposits composed of classical turbidites are commonly distributed at the distal ends of minor channels (Posamentier and Walker, 2006).

6. Depositional history

The Bac Thuy Formation consists of a large-scale deepening-upward sequence of deposits from a tidal flat and wave-influenced shallow platform (Facies Association A) to a slope (Facies Association B) and finally to a marginal basin plain (Facies Association C), indicating an overall transgressive environment. The slope and marginal basin deposits are over 50 m thick and dominate the formation. The tidal flat and shallow platform carbonates are thin–only approximately 4 m thick–at KC01. During our preliminary research at the type section of the Bac Thuy Formation, we found no exposures of these tidal flat deposits (Komatsu et al., 2011).

At KC01, at least four small-scale shallowing-upward sequences (PS1–PS4) bounded by major marine flooding surfaces were recognized in the shallow marine succession (Fig. 6). These small-scale shallowing-upward sequences represent typical parasequence sets. PS1 and PS2 begin with wave-influenced shallow platform carbonates containing many well-preserved marine shells, such as ammonoids and conodonts, and end with supra- to intertidal deposits. Relatively thick supra- to intertidal deposits dominate in the upper part of PS1; in contrast, tidal deposits in the upper part of PS2 are thin and show no evidence of desiccation cracks, which if present would indicate a supratidal facies. PS3 and PS4 consist of conspicuous basal intraclastic carbonates and wave-influenced shallow platform carbonates containing common marine fossils. The basal intraclastic carbonates, which are characterized by a clast-supported fabric and erosive basal surfaces, are interpreted as transgressive lag deposits. The erosive surfaces may represent marine flooding surfaces. One of these possible marine flooding surfaces corresponds to the basal surface of the tidal channel deposits in PS2 (Fig. 7A). The parasequence stacking pattern (PS1–PS4) is retrogradational, meaning that the facies at the top of each parasequence becomes progressively more distal. This retrogradational parasequence set, consisting of cyclic wave-influenced shallow platform carbonate tidal flat deposits, is interpreted as part of a transgressive sequence. It is covered by thick slope deposits composed of limestone breccia beds with typical erosive basal surfaces. The erosive surfaces may represent major marine flooding surfaces around the carbonate platform margin.

Lehrmann et al. (2007a) reported high subsidence rates in the southern part of the Early Triassic Nanpanjiang basin resulting from the convergence of the South China and Indochina plates during the Indosinian orogeny. In the An Chau basin, it is likely that facies distributions, stacking patterns, and subsidence rates were strongly controlled by local tectonics in the eastern Tethys seaway. The thick, large-scale deepening-upward sequence containing small-scale shallowing-upward sequences (parasequence sets) was likely generated by repeated local tectonic subsidence events, rather than by eustatic sea level fluctuation.

7. Siliciclastic influx into the southern Nanpanjiang basin

The shallow marine facies of the Early to Middle Triassic were dominated by carbonates of the Yangtze platform and several other isolated platforms on the South China block (Lehrmann et al., 1998, 2001, 2003; Enos et al., 2006; Lehrmann et al., 2007a,b; Collin et al., 2009; Li et al., 2012). These shallow marine deposits are characterized by wave- and storm-dominated carbonates (Bao, 1998) and tide-influenced reef interior deposits (Lehrmann et al., 2003, 2007a,b; Li et al., 2012). According to Lehrmann et al. (2007a,b), the isolated Induan to early Olenekian Chongzuo-Pingguo platform in southwestern Guangxi Province (adjacent to Lang Son Province) is composed mainly of oolitic, bioclastic, and intraclastic limestones, dolomite, and marl, which developed from a low-relief bank rimmed with ooid shoals. The tidal flat facies of this platform consists of cross-bedded grainstone and flaser to lenticular bedding with mud drapes and desiccation cracks. The surrounding slope and basin systems consist of thick hemipelagic mudstone and gravity flow deposits such as limestone breccias and turbidites. The southern margin of the Chongzuo-Pingguo platform is defined in the Chongzuo area by the east–west-striking Pingxiang-Dongmen fault, as evidenced by the presence of shallow marine deposits north of the fault and basinal deposits south of the fault.

During the early Olenekian, the An Chau basin in Vietnam filled mainly with the shallow marine siliciclastics of the Lang Son Formation and the fossiliferous shallow marine carbonates and slope deposits (limestone breccia, hemipelagic mudstone) of the Bac Thuy Formation. The shallow marine deposits of the Induan to early Olenekian Lang Son Formation are composed of shelf mudstone and shoreface sandstone with wave ripples and HCS (Komatsu et al., 2006; Komatsu and Dang, 2007). The lower Olenekian Bac Thuy Formation is characterized by tidal deposits (Facies Association A), which consist of tidal bundles intercalated by mud drapes and lenticular to flaser beds, and fossiliferous carbonates with wave ripples. Therefore, tide- and wave-influenced siliciclastic and carbonate facies dominate the early Olenekian in the An Chau basin in Vietnam, whereas the shallow marine facies in South China is dominated by carbonates.

The Olenekian slope and marginal basin plain deposits in the An Chau and Nanpanjiang basins consist mainly of siliciclastic and calcareous gravity flow deposits and hemipelagic mudstone. In particular, the Lower Triassic Luolou Formation in South China is primarily composed of limestone breccia, calcareous and siliciclastic turbidites, and hemipelagite (Lehrmann et al., 2007a,b; Galfetti et al., 2008). According to Lehrmann et al. (2007a), who examined long-term subsidence patterns during the Proterozoic to Triassic, the Yangtze platform and other, isolated platforms – including the Chongzuo-Pingguo platform and the Great Bank of Guizhou – were characterized by high subsidence

and sedimentation rates during the Olenekian to Anisian in the Chongzuo area; peak subsidence rates occurred earlier in the southern basin (i.e., in the Pingguo and Chongzuo areas) than in the northern basin. During the Olenekian to Anisian, in the Nanpanjiang basin the huge accommodation space was filled with carbonate and siliciclastic gravity flow deposits. However, the timing and source area of the siliciclastic gravity flows in the southern Nanpanjiang basin are poorly understood, although Enos et al. (2006) suggested that the Middle Triassic turbidites originated from the east in association with the Jiangnan uplift in the northern basin.

In contrast, Lower Triassic siliciclastic sediments are common in the shallow to deep marine facies in the An Chau basin. Thick siliciclastic slump deposits accumulated in a slope environment are intercalated within the upper part of the Induan to early Olenekian Lang Son Formation. Many turbidite beds consisting of siliciclastics are embedded in the Olenekian Bac Thuy Formation. These observations suggest that the Lower Triassic siliciclastic sediments in the southern Nanpanjiang basin originated mainly from the shelf in the An Chau basin or from a landmass in northern Vietnam. Climbing-ripple and current-ripple laminations in high- and low-density marginal basin turbidites indicate eastward, northeastward, and southeastward paleocurrent directions in the Bac Thuy Formation (Fig. 3). In addition, Zhang (1986) inferred that paleocurrents flowed from the south on the basis of data from the gravity-flow deposits in the Middle Triassic basin fill in Guangxi Province.

8. Latest Smithian low-diversity fauna in anoxic to dysoxic facies

Intense oceanic anoxic events affected end-Permian to Early Triassic environments, the end-Permian mass extinction, the Smithian–Spathian boundary event, and recoveries of marine benthic animals (Hallam, 1991; Wignall and Hallam, 1992; Hallam and Wignall, 1997; Isozaki, 1997; Wignall and Twitchett, 2002; Brayard et al., 2006; Galfetti et al., 2007, 2008; Payne et al., 2011; Payne and Clapham, 2012). Organic-rich dark gray to black shale and mudstone with monospecific fossil assemblages and no evidence of bioturbation, as well as considerable biological and biochemical data indicating anoxic events during the Olenekian, have been reported (Galfetti et al., 2008; Payne et al., 2011; Song et al., 2012). Organic-rich deposits (Facies 8), which suggest anoxic to dysoxic conditions, accumulated mainly in the latest Smithian marginal basin environments in the An Chau basin, though the top of Facies 8 contains the Smithian–Spathian boundary. Facies 8 is characterized by monospecific conodont, ammonoid, and bivalve assemblages. Only one conodont species, *Neospathodus pingdingshanensis* (Zhao and Orchard) (i.e., *Novispathodus pingdingshanensis* (Zhao and Orchard); Goudemand et al., 2012), is present in the organic-rich dark gray limestone (Komatsu et al., 2011; Maekawa et al., 2012). In contrast, Thang (1989) reported a Smithian conodont assemblage consisting of many conodont species, including *Neospathodus waageni*, *Platyvillosus costatus* (Staesche), and *Neospathodus dieneri* (Sweet), from bioclastic limestones in the type section of the Bac Thuy Formation. In a preliminary report, Maekawa et al. (2012) reported a *Neospathodus waageni* assemblage from the lower Bac Thuy Formation (Facies 1b, 3, and 4 in the KC01 and KC02 sections in this study) and a typical lower Spathian conodont assemblage composed of *Icriospathodus collinsoni* (Solien), *Neospathodus triangularis* (Bender), and *Triassospathodus homeri* (Bender) from the upper Bac Thuy Formation (Facies 10 in the KC02, NT01, and BR01 sections). A diversified ammonoid assemblage consisting of *Owenites*, *Paranannites*, *Ussuria*, *Preflorianites*, and *Anaflemingites* co-occurs in this formation with a *Neospathodus waageni* assemblage (Komatsu et al., 2011; Maekawa et al., 2012), whereas the organic-rich deposits (Facies 8 in the KC02, NT01, and BR01 sections) bear only *X. variocostatus* (Komatsu et al., 2013). The weakly bioturbated mudstone (Facies 10) overlying Facies 8 commonly includes several types of Spathian ammonoids such as *Tirolites*, *Columbites*, and *Xenoceltites* (Komatsu et al., 2011, 2013). In addition, Komatsu et al. (2011, 2013) reported that benthic mollusks in Facies 8 occur in low-diversity thin-shelled epifaunal bivalve assemblages dominated by *Crittendenia*. Infaunal bivalves and gastropods are rare. Microfossils are also low in diversity; the assemblages are monospecific and composed of small, poorly ornamented ostracods (*Propontcypris*) and a few species of spheroidal radiolarians (Spumellaria).

In Guangxi Province, South China, the *Xenoceltites* beds in upper Unit IV of the Luolou Formation are characterized by pyrite aggregates and laminated organic-rich limestone and shale devoid of bioturbation, suggesting low-energy deposition and some environmental stress such as oxygen deficiency (Galfetti et al., 2008). According to Galfetti et al. (2008), two anoxic events during the Olenekian, evidenced by organic- and pyrite-rich black shales, are invariably identified in deposits underlying the basal Smithian (*Kashmirites densistriatus* ammonoid beds) and in the uppermost Smithian (*Anasibirites multiformis* ammonoid beds). Song et al. (2012) noted the occurrence of two intense oceanic anoxic events during the Olenekian, a Smithian–earliest Spathian event and a mid-Spathian event, on the basis of conodont redox data (Ce anomalies and Th/U ratios in conodont albid crown apatite material). Although some nektonic taxa such as ammonoids and conodonts recovered rapidly from the end-Permian mass extinction and diversified from the Induan to the early Olenekian, global ammonoid and conodont extinction events are known to have occurred during the latest Smithian (Hallam, 1991; Brayard et al., 2006; Galfetti et al., 2007; Orchard, 2007; Galfetti et al., 2008; Orchard, 2010; Payne et al., 2011; Hofmann et al., in press). Near the end of the Smithian in the Lower Triassic, ammonoid diversity dropped globally (Brayard et al., 2006). During conodont radiation, the compositions of Spathian conodont assemblages changed drastically from those of the Smithian (Orchard, 2007). These extinction events and faunal changes likely were related to or resulted from oceanic anoxic events during the Smithian. Modern slope and marginal basin environments often become depleted in dissolved oxygen in response to changes like those observed in the paleoceanographic record, such as increased surface ocean productivity and stagnation of vertical mixing (e.g., Arthur and Sageman, 1994). Benthic and planktonic species compositions were likely also affected by such paleoceanographic changes. Although the compositions of Olenekian mega- and microfossil faunal assemblages in the Bac Thuy Formation have been studied only preliminarily, further investigation of detailed faunal changes in the An Chau basin may improve our understanding of the latest Smithian anoxic events and the evolutionary history of Lower Triassic marine organisms in the eastern Tethys seaway.

9. Conclusions

1. In the An Chau basin, northeastern Vietnam, the Olenekian stage consists of shallow marine to marginal basin plain mixed carbonate and siliciclastic deposits. The upper Lang Son Formation is dominated by siliciclastic facies composed of storm- and wave-influenced shallow marine and slope deposits. The overlying and interfingering Bac Thuy Formation is a typical deepening-upward sequence of fossiliferous carbonates and siliciclastics, consisting of tidal flat, wave-influenced carbonate platform, slope, and marginal basin plain deposits.
2. The Smithian–Spathian boundary, which is defined by the first appearance of *Tirolites* (ammonoid), and latest Smithian–earliest Spathian anoxic to dysoxic facies are intercalated within the succession of slope to marginal basin plain facies. The anoxic to dysoxic facies show no evidence of bioturbation and are characterized by low-diversity ammonoid, bivalve, and conodont assemblages.
3. Paleocurrent indicators in the siliciclastic gravity flow deposits suggest that paleocurrent directions were approximately eastward

during the earliest Spathian. Thus, the siliciclastics that accumulated in the southern Nanpanjiang basin were likely supplied from the west.

Acknowledgements

We thank T. Kumagae (Japan Petroleum Exploration Co., Ltd.) and H. Matsuda (Kumamoto University) for their useful discussion on the Lower Triassic stratigraphy and carbonate sedimentology. We are also indebted to two referees, Michael Hautmann (Universität Zürich) and Akihiro Misaki (Kitakyushu Museum of Natural History and Human History), for critical revisions. This study was partly supported by grants-in-aid from the Japanese Ministry of Education, Culture, Sports, Science, and Technology (20740300 to T. Komatsu), Japan Society for Promotion of Science (25400500 to T. Komatsu), the JSPS-VAST Joint Research Program, and a HIR grant UM.C/625/1/HIR/140 from the University of Malaya (to M. Sone).

References

Aigner, T., 1982. Calcareous tempestites: storm-dominated stratification, Upper Muschelkalk limestones (Middle Triassic, SW Germany). In: Einsele, G., Seilacher, A. (Eds.), Cyclic and Event Stratification. Springer-Verlag, Berlin, pp. 180–189.

Arnott, R.W.C., 2010. Deep-marine sediments and sedimentary systems. In: James, N.P., Dalrymple, R.W. (Eds.), Facies models 4. Geological Association of Canada, Ontario, pp. 295–322.

Arthur, M.A., Sageman, B.B., 1994. Marine black shales: depositional mechanisms and environments of ancient deposits. Annual Review of Earth and Planetary Sciences 22, 499–551.

Bao, Z., 1998. Continental slope limestones of Lower and Middle Triassic, South China. Sedimentary Geology 118, 77–93.

Boersma, J.R., Terwindt, J.H.J., 1981. Neap-spring tide sequences of intertidal shoal deposits in a mesotidal estuary. Sedimentology 28, 151–170.

Bouma, A.H., 1962. Sedimentology of Some Flysch Deposits: a Graphic Approach to Facies Interpretation. Elsevier, Amsterdam (168 pp.).

Brayard, A., Bucher, H., 2008. Smithian (Early Triassic) ammonoid faunas from northwestern Guangxi (South China): taxonomy and biochronology. Fossils and Strata 55, 1–179.

Brayard, A., Bucher, H., Escarguel, G., Fluteau, F., Bourquin, S., Galfetti, T., 2006. The Early Triassic ammonoid recovery: paleoclimatic significance of diversity gradients. Palaeogeography, Palaeoclimatology, Palaeoecology 239, 374–395.

Bromley, R.G., 1996. Trace fossils. Biology, Taphonomy and Applications.Chapman and Hall, London (361 pp.).

Chakrabarti, A., 2005. Sedimentary structures of tidal flats: a journey from coast to inner estuarine region of eastern India. Journal of Earth System Science 114, 353–368.

Collin, P.Y., Kershaw, S., Crasquin-Soleau, S., Feng, Q.L., 2009. Facies changes and diagenetic processes across the Permian–Triassic boundary event horizon, Great Bank of Guizhou, south China: a controversy of erosion and dissolution. Sedimentology 56, 677–693.

Dalrymple, R.W., 1992. Tidal depositional systems. In: Walker, R.G., James, N.P. (Eds.), Facies Models: Response to Sea Level Change. Geological Association of Canada, Ontario, pp. 195–218.

Dalrymple, R.W., 2010. Tidal depositional systems. In: James, N.P., Dalrymple, R.W. (Eds.), Facies Models 4. Geological Association of Canada, Ontario, pp. 201–232.

Dalrymple, R.W., Choi, K., 2007. Morphologic and facies trends through the fluvial-marine transition in tide-dominated depositional systems: a systematic framework for environmental and sequence-stratigraphic interpretation. Earth-Science Reviews 81, 135–174.

Dang, T.H., 1998. Stratigraphical and paleontological data on Lower Triassic sediments in the Song Hien structure-facies zone. Geology and Mineral Resources 6, 21–34 (in Vietnamese with English abstract).

Dang, T.H., 2006. Mesozoic. In: Thanh, T.D. (Ed.), Stratigraphic Units of Vietnam. Vietnam National University Publishing House, Hanoi, pp. 245–366.

Dang, T.H., Nguyen, D.H., 2005. Fossil zones and stratigraphic correlation of the Lower Triassic sediments of East Bac Bo. Journal of Geology, Series A 11–12, 1–9.

Davis, R.A., 2012. Tidal signatures and their preservation potential in stratigraphic sequences. In: Davis, R.A., Dalrymple, R.W. (Eds.), Principles of Tidal Sedimentology. Springer, Dordrecht, pp. 35–56.

Ekdale, A.A., Mason, T.R., 1988. Characteristic trace fossil associations in oxygen-poor sedimentary environments. Geology 16, 720–723.

Enos, P., Lehrmann, D.J., Jiayong, W., Youyi, Y., Jiafei, X., Chaikin, D.H., Minzoni, M., Berry, A.K., Montgomery, P., 2006. Triassic evolution of the Yangtze Platform in Guizhou Province, People's Republic of China. The Geological Society of America, Special Paper 417 (Boulder, Colorado, 105 pp.).

Flemming, B.W., 2012. Siliciclastic back-barrier tidal flat. In: Davis, R.A., Dalrymple, R.W. (Eds.), Principles of Tidal Sedimentology. Springer, Dordrecht, pp. 231–267.

Friedman, G.M., Chakraborty, C., 2006. Interpretation of tidal bundles: two reasons for a paradigm shift. Carbonates and Evaporites 21, 170–175.

Galfetti, T., Hochuli, P.A., Brayard, A., Bucher, H., Weissert, H., Vigran, J.O., 2007. Smithian–Spathian boundary event: evidence for global climatic change in the wake of the end-Permian biotic crisis. Geology 35, 291–294.

Galfetti, T., Bucher, H., Martini, R., Hochuli, P.A., Weissert, H., Crasquin-Soleau, S., Brayard, A., Goudemand, N., Brühwiler, T., Guodun, K., 2008. Evolution of Early Triassic outer platform paleoenvironments in the Nanpanjiang Basin (South China) and their significance for the biotic recovery. Sedimentary Geology 204, 36–60.

Goudemand, N., Orchard, M.J., Tafforeau, P., Urdy, S., Brühwiler, T., Brayard, A., Galfetti, T., Bucher, H., 2012. Early Triassic conodont clusters from South China: revision of the architecture of the 15 element apparatuses of the superfamily Gondolelloidea. Palaeontology 55, 1021–1034.

Hallam, A., 1991. Why was there a delayed radiation after the end-Palaeozoic extinctions? Historical Biology 5, 257–262.

Hallam, A., Wignall, P., 1997. Mass Extinctions and Their Aftermath. Oxford University Press, Oxford (320 pp.).

Hiscott, R.N., 1994. Traction-carpet stratification in turbidites—fact or fiction? Journal of Sedimentary Research A64, 204–208.

Hodgson, D.M., Flint, S.S., 2005. Submarine slope systems: processes and products. Geological Society Special Publication, 224. Geological Society, London (225 pp.).

Hofmann, R., Hautmann, M., Brayard, A., Nützel, A., Bylund, G.K., Jenks, F.J., Vennin, E., Olivier, N., Bucher, H., 2013. Recovery of benthic marine communities from the end-Permian mass extinction at the low latitudes of eastern Panthalassa. Palaeontology (in press).

Isozaki, Y., 1997. Permo-Triassic boundary superanoxia and stratified superocean: records from lost deep sea. Science 276, 235–238.

Janson, X., Kerans, C., Loucks, R., Marhx, M.A., Reyes, C., Murguia, F., 2011. Seismic architecture of a Lower Cretaceous platform-to-slope system, Santa Agueda and Poza Rica fields, Mexico. The American Association of Petroleum Geologists Bulletin 95, 105–146.

Johnson, A.M., 1970. Physical Processes in Geology. Freeman, San Francisco (571 pp.).

Johnson, H.D., Boldwin, C.T., 1996. Shallow clastic seas, In: Reading, H.D. (Ed.), Sedimentary Environments, Processes, Facies and Stratigraphy, Third Edition. Blackwell, Oxford, pp. 232–280.

Khuc, Vu, 1984. Triassic Ammonoids in Vietnam. General Department of Geology of SR Vietnam, Hanoi (136 pp., in Vietnamese).

Khuc, Vu, 1991. Paleontological atlas of Vietnam. Mollusca, vol. 3. Science and Technics Publishing House, Hanoi (207 pp.).

Khuc, Vu, Dagyx, A.X., Kiparisova, L.D., Nguyen, B.N., Truong, C.B., Srebrodolskaia, I.N., 1965. Characteristic Fossils of Triassic of North Vietnam. General Department of Geology of DR Vietnam, Hanoi (118 pp., in Vietnamese and French).

Kidwell, S.M., Fürsich, F.T., Aigner, T., 1986. Conceptual framework for the analysis and classification of fossil concentration. Palaios 1, 228–238.

Komatsu, T., Dang, T.H., 2007. Lower Triassic bivalve fossils from the Song Da and An Chau Basins, North Vietnam. Paleontological Research 11, 135–144.

Komatsu, T., Chen, J., Cao, M., Stiller, F., Naruse, H., 2004. Middle Triassic (Anisian) diversified bivalves: depositional environments and bivalve assemblages in the Leidapo Member of the Qingyan Formation, southern China. Palaeogeography, Palaeoclimatology, Palaeoecology 208, 207–223.

Komatsu, T., Dang, T.H., Chen, J.H., 2006. Depositional environments and fossil bivalves in lowermost parts of the Lower Triassic Systems in North Vietnam and South China. Journal of Geography 115, 470–483 (in Japanese with English abstract).

Komatsu, T., Dang, T.H., Chen, J.H., 2008a. Lower Triassic bivalve assemblages after the end-Permian mass extinction in South China and North Vietnam. Paleontological Research 12, 119–128.

Komatsu, T., Ono, M., Naruse, H., Kumagae, T., 2008b. Upper Cretaceous depositional environments and bivalve assemblage of far-east Asia: the Himenoura Group, Kyushu, Japan. Cretaceous Research 29, 489–508.

Komatsu, T., Dang, T.H., Nguyen, D.H., 2010. Radiation of Middle Triassic bivalve: bivalve assemblages characterized by infaunal and semi-infaunal burrowers in a storm- and wave-dominated shelf, An Chau Basin, North Vietnam. Palaeogeography, Palaeoclimatology, Palaeoecology 291, 190–204.

Komatsu, T., Maekawa, T., Shigeta, Y., Dang, T.H., Nguyen, D.H., 2011. Lower Triassic stratigraphy and fossils in North Vietnam (a preliminary work). Abstracts with Programs, the 2011 Annual Meeting, the Palaeontological Society of Japan, July 1–3, 2011.Ishikawa Prefecture, Kanazawa 26 (in Japanese).

Komatsu, T., Shigeta, Y., Dang, T.H., Nguyen, D.H., Dinh, C.T., Maekawa, T., Tanaka, G., 2013. *Crittendenia* (Bivalvia) from the Lower Triassic Olenekian Bac Thuy Formation, An Chau Basin, Northern Vietnam. Paleontological Research 17, 1–11.

Lehrmann, D.J., Wei, J., Enos, P., 1998. Controls on facies architecture of a large Triassic carbonate platform: the Great Bank of Guizhou, Nanpanjiang Basin, South China. Journal of Sedimentary Research 68, 311–326.

Lehrmann, D.J., Wang, W., Wei, J., Yu, Y., Xiao, J., 2001. Lower Triassic peritidal cyclic limestone: an example of anachronistic carbonate facies from the Great Bank of Guizhou, Nanpanjiang Basin, Guizhou Province, South China. Palaeogeography, Palaeoclimatology, Palaeoecology 173, 103–123.

Lehrmann, D.J., Payne, J.L., Felix, S.V., Dillett, P.M., Wang, H., Yu, Y., Wei, J., 2003. Permian-Triassic boundary sections from shallow-marine carbonate platforms of the Nanpanjiang Basin, South China: implications for oceanic conditions associated with the end-Permian extinction and its aftermath. Palaios 18, 138–152.

Lehrmann, D.J., Payne, J.L., Pei, D., Enos, P., Druke, D., Steffen, K., Zhang, J., Wei, J., Orchard, M.J., Ellwood, B., 2007a. Record of the end-Permian extinction and Triassic biotic recovery in the Chongzuo-Pingguo platform, southern Nanpanjiang basin, Guangxi, south China. Palaeogeography, Palaeoclimatology, Palaeoecology 252, 200–217.

Lehrmann, D.J., Donghong, P., Enos, P., Minzoni, M., Ellwood, B.B., Orchard, M.J., Jiyan, Z., Jiayong, W., Dillett, P., Koenig, J., Steffen, K., Druke, D., Druke, J., Kessel, B., Newkirk, T., 2007b. Impact of differential tectonic subsidence on isolated carbonate-platform

evolution: Triassic of the Nanpanjiang Basin, south China. The American Association of Petroleum Geologists Bulletin 91, 287–320.
Li, X., Yu, M., Lehrmann, D.J., Payne, J.L., Pei, D., Kelly, B.M., Minzoni, M., 2012. Factors controlling carbonate platform asymmetry: preliminary results from the Great Bank of Guizhou, an isolated Permian-Triassic Platform in the Nanpanjiang basin, south China. Palaeogeography, Palaeoclimatology, Palaeoecology 315, 158–171.
Lowe, D.R., 1979. Sediment gravity flows: their classification and some problems of application to natural flows and deposits. In: Doyle, L.J., Pilkey, O.H. (Eds.), Geology of Continental Slopes. SEPM, Special Publication, 27. Society for Sedimentary Geology, Tulsa, Oklahoma, pp. 75–82.
Lowe, D.R., 1982. Sediment gravity flows: II. Depositional models with special reference to the deposits of high-density turbidity currents. Journal of Sedimentary Petrology 52, 279–297.
Maeda, H., Shigeta, Y., 2009. Ammonoid mode of occurrence. In: Shigeta, Y., Zakharov, Y.D., Maeda, H., Popov, A.M. (Eds.), The Lower Triassic System in the Abrek Bay area, South Primorye, Russia. National Museum of Nature and Science Monographs, 38. National Museum of Nature and Science, Tokyo, pp. 36–38.
Maekawa, T., Komatsu, T., Shigeta, Y., Dang, T.H., Nguyen, D.H., 2012. Biostratigraphy of the Lower Triassic Bac Thuy Formation in Lang Son area, Northern Vietnam. Abstracts with Programs, the 2012 Annual Meeting, the Palaeontological Society of Japan, June 29–July 1, 2012. Aichi Prefecture, Nagoya, p. 35 (in Japanese).
Maekawa, T., Komatsu, T., Shigeta, Y., Dang, T.H., 2013. Conodonts and geological age of the upper part of the Lang Son Formation distributed in northeastern Vietnam. Abstracts with Programs, the 2013 Annual Meeting, the Palaeontological Society of Japan, January 25–27, 2013. Kanagawa Prefecture, Yokohama, p. 35 (in Japanese).
Metcalfe, I., 1998. Palaeozoic and Mesozoic geological evolution of the SE Asian region: multidisciplinary constraints and implications for biogeography. In: Hall, R., Holloway, J.D. (Eds.), Biogeography and Geological Evolution of SE Asia. Backhuys Publishers, Leiden, pp. 25–41.
Metcalfe, I., 2009. Late Palaeozoic and Mesozoic tectonic and palaeogeographical evolution SE Asia. In: Buffetaut, E., Cuny, G., Le Loeuff, J., Suteethorn, V. (Eds.), Late Palaeozoic and Mesozoic Ecosystems in SE Asia. The Geological Society, London, Special Publications, 315, pp. 7–23.
Mulder, T., 2011. Gravity processes and deposits on continental slope, rise and abyssal plains. In: Hüneke, H., Mulder, T. (Eds.), Deep-Sea Sediments, pp. 25–148.
Mulder, T., Alexander, J., 2001. The physical character of sedimentary density currents and their deposits. Sedimentology 48, 269–299.
Mullins, H., Cook, H.E., 1986. Carbonate apron models: alternatives to the submarine fan model for paleoenvironmental analysis and hydrocarbon exploration. Sedimentary Geology 48, 37–79.
Orchard, M.J., 2007. Conodont diversity and evolution through the latest Permian and Early Triassic upheavals. Palaeogeography, Palaeoclimatology, Palaeoecology 252, 93–117.
Orchard, M.J., 2010. Triassic conodonts and their role in stage boundary definition. In: Lucas, S.G. (Ed.), The Triassic Timescale. Geological Society, London, Special Publications, 334, pp. 139–161.
Payne, J.L., Clapham, M.E., 2012. End-Permian mass extinction in the oceans: an ancient analog for the twenty-first century? The Annual Review of Earth and Planetary Sciences 40, 89–111.
Payne, J.L., Summers, M., Rego, B.L., Altiner, D., Wei, J., Yu, M., Lehrmann, D.J., 2011. Early and Middle Triassic trends in diversity, evenness, and size of foraminifers on a carbonate platform in south China: implications for tempo and mode of biotic recovery from the end-Permian mass extinction. Paleobiology 37, 409–425.
Payros, A., Pujalte, V., Orue-Etxebarria, X., 2007. A point-sourced calciclastic submarine fan complex (Eocene Anotz Formation, western Pyrenees): facies architecture, evolution and controlling factors. Sedimentology 54, 137–168.
Playton, T.E., Janson, X., Kerans, C., 2010. Carbonate slopes. In: James, N.P., Dalrymple, R.W. (Eds.), Facies Models 4. Geological Association of Canada, Ontario, pp. 449–476.
Posamentier, H.W., Kolla, V., 2003. Geomorphology and stratigraphy of depositional elements in deep-water settings. Journal of Sedimentary Research 73, 367–388.
Posamentier, H.W., Walker, R.G., 2006. Facies models revisited. SEPM Special Publication 84 (Tulsa, Oklahoma, 531 pp.).
Postma, G., Nemec, W., Zachariasse, W.J., 1988. Large floating clasts in turbidites: a mechanism for their emplacement. Sedimentary Geology 58, 47–61.
Pratt, B.R., 2010. Peritidal carbonates. In: James, N.P., Dalrymple, R.W. (Eds.), Facies Models 4. Geological Association of Canada, Ontario, pp. 401–420.
Pratt, B.R., James, N.P., Cowan, C.A., 1992. Peritidal carbonates. In: Walker, R.G., James, N.P. (Eds.), Facies Models: Response to Sea Level Change. Geological Association of Canada, Ontario, pp. 303–322.
Prior, D.B., Bornhold, B.D., Coleman, J.M., Bryant, W.R., 1982. Morphology of a submarine slide, Kitimat arm, British Columbia. Geology 10, 588–592.
Reading, H.G., Collinson, J.D., 1996. Clastic coasts. In: Reading, H.G. (Ed.), Sedimentary Environments, Processes, Facies and Stratigraphy. Blackwell Science, Oxford, pp. 154–231.
Sohn, Y.K., 1997. On traction-carpet sedimentation. Journal of Sedimentary Research 67, 502–509.
Sohn, Y.K., Choe, M.Y., Jo, H.R., 2002. Transition from debris flow to hyperconcentrated flow in a submarine channel (the Cretaceous Cerro Toro Formation, southern Chile). Terra Nova 14, 405–415.
Song, H., Wignall, P.B., Tong, J., Bond, D.P.G., Song, H., Lai, X., Zhang, K., Wang, H., Chen, Y., 2012. Geochemical evidence from bio-apatite for multiple oceanic anoxic events during Permian–Triassic transition and the link with end-Permian extinction and recovery. Earth and Planetary Science Letters 353–354, 12–21.
Stow, D.A.V., Reading, H.G., Collinson, J.D., 1996. Deep seas. In: Reading, H.G. (Ed.), Sedimentary Environments, Processes, Facies and Stratigraphy. Blackwell Science, Oxford, pp. 395–453.
Thang, B.D., 1989. Lower Triassic conodonts from North Vietnam. Acta Palaeontologica Polonica 34, 391–416.
Tucker, M.E., 1991. Sedimentary Petrology, an Introduction to the Origin of Sedimentary Rocks. Blackwell Scientific Publications, Oxford (260 pp.).
Tucker, M.E., Wright, V.P., 1990. Carbonate Sedimentology. Blackwell, Oxford (482 pp.).
Van den Berg, J.H., Boersma, J.R., Van Gelder, A., 2007. Diagnostic sedimentary structures of the fluvial-tidal transition zone — evidence from deposits of the Rhine and Meuse. Netherlands Journal of Geosciences 86, 287–306.
Walker, R.G., 1985. Mudstones and thin-bedded turbidites associated with the Upper Cretaceous Wheeler Gorge conglomerates, California: a possible channel-levee complex. Journal of Sedimentary Petrology 55, 279–290.
Walker, R.G., 1992. Turbidites and submarine fans. In: Walker, R.G., James, N.P. (Eds.), Facies Models: Response to Sea Level Change. Geological Association of Canada, Ontario, pp. 239–263.
Wignall, P.B., Hallam, A., 1992. Anoxia as a cause of the Permian/Triassic mass extinction: facies evidence from northern Italy and the western United States. Palaeogeography, Palaeoclimatology, Palaeoecology 93, 21–46.
Wignall, P.B., Twitchett, R.J., 2002. Extent, duration and nature of the Permian-Triassic superanoxic event. Geological Society of America, Special Paper 356, 395–413.
Wright, V.P., 1990. Peritidal carbonates. In: Tucker, M.E., Wright, V.P. (Eds.), Carbonate Sedimentology. Blackwell Science, Oxford, pp. 137–164.
Wright, V.P., Burchette, 1996. Shallow-water carbonate environments. In: Reading, H.G. (Ed.), Sedimentary Environments: Processes, Facies and Stratigraphy. Blackwell Science, Oxford, pp. 325–392.
Yang, C.S., Nio, S.W., 1985. The estimation of palaeohydrodynamic processes from subtidal deposits using time series analysis methods. Sedimentology 32, 41–57.
Zhang, J., 1986. Middle Triassic gravity-flow deposits in western Guangxi: Regional Geology of China. 5, 125–132.